IEC TR 62681

Edition 2.0 2022-05

TECHNICAL REPORT

colour inside

Electromagnetic performance of high voltage direct current (HVDC) overhead transmission lines

IEC TR 62681:2022-05(en)

IEC Secretariat
3, rue de Varembé
CH-1211 Geneva 20
Switzerland

Tel.: +41 22 919 02 11
info@iec.ch
www.iec.ch

About the IEC
The International Electrotechnical Commission (IEC) is the leading global organization that prepares and publishes International Standards for all electrical, electronic and related technologies.

About IEC publications
The technical content of IEC publications is kept under constant review by the IEC. Please make sure that you have the latest edition, a corrigendum or an amendment might have been published.

IEC publications search - webstore.iec.ch/advsearchform
The advanced search enables to find IEC publications by a variety of criteria (reference number, text, technical committee, …). It also gives information on projects, replaced and withdrawn publications.

IEC Just Published - webstore.iec.ch/justpublished
Stay up to date on all new IEC publications. Just Published details all new publications released. Available online and once a month by email.

IEC Customer Service Centre - webstore.iec.ch/csc
If you wish to give us your feedback on this publication or need further assistance, please contact the Customer Service Centre: sales@iec.ch.

IEC Products & Services Portal - products.iec.ch
Discover our powerful search engine and read freely all the publications previews. With a subscription you will always have access to up to date content tailored to your needs.

Electropedia - www.electropedia.org
The world's leading online dictionary on electrotechnology, containing more than 22 300 terminological entries in English and French, with equivalent terms in 19 additional languages. Also known as the International Electrotechnical Vocabulary (IEV) online.

IEC TR 62681

Edition 2.0 2022-05

TECHNICAL REPORT

colour inside

Electromagnetic performance of high voltage direct current (HVDC) overhead transmission lines

INTERNATIONAL
ELECTROTECHNICAL
COMMISSION

ICS 29.240.20

ISBN 978-2-8322-3130-2

Warning! Make sure that you obtained this publication from an authorized distributor.

CONTENTS

INTERNATIONAL ELECTROTECHNICAL COMMISSION

_____

ELECTROMAGNETIC PERFORMANCE OF HIGH VOLTAGE DIRECT CURRENT (HVDC) OVERHEAD TRANSMISSION LINES

FOREWORD

1) The International Electrotechnical Commission (IEC) is a worldwide organization for standardization comprising all national electrotechnical committees (IEC National Committees). The object of IEC is to promote international co-operation on all questions concerning standardization in the electrical and electronic fields. To this end and in addition to other activities, IEC publishes International Standards, Technical Specifications, Technical Reports, Publicly Available Specifications (PAS) and Guides (hereafter referred to as "IEC Publication(s)"). Their preparation is entrusted to technical committees; any IEC National Committee interested in the subject dealt with may participate in this preparatory work. International, governmental and non-governmental organizations liaising with the IEC also participate in this preparation. IEC collaborates closely with the International Organization for Standardization (ISO) in accordance with conditions determined by agreement between the two organizations.
2) The formal decisions or agreements of IEC on technical matters express, as nearly as possible, an international consensus of opinion on the relevant subjects since each technical committee has representation from all interested IEC National Committees.
3) IEC Publications have the form of recommendations for international use and are accepted by IEC National Committees in that sense. While all reasonable efforts are made to ensure that the technical content of IEC Publications is accurate, IEC cannot be held responsible for the way in which they are used or for any misinterpretation by any end user.
4) In order to promote international uniformity, IEC National Committees undertake to apply IEC Publications transparently to the maximum extent possible in their national and regional publications. Any divergence between any IEC Publication and the corresponding national or regional publication shall be clearly indicated in the latter.
5) IEC itself does not provide any attestation of conformity. Independent certification bodies provide conformity assessment services and, in some areas, access to IEC marks of conformity. IEC is not responsible for any services carried out by independent certification bodies.
6) All users should ensure that they have the latest edition of this publication.
7) No liability shall attach to IEC or its directors, employees, servants or agents including individual experts and members of its technical committees and IEC National Committees for any personal injury, property damage or other damage of any nature whatsoever, whether direct or indirect, or for costs (including legal fees) and expenses arising out of the publication, use of, or reliance upon, this IEC Publication or any other IEC Publications.
8) Attention is drawn to the Normative references cited in this publication. Use of the referenced publications is indispensable for the correct application of this publication.
9) Attention is drawn to the possibility that some of the elements of this IEC Publication may be the subject of patent rights. IEC shall not be held responsible for identifying any or all such patent rights.

IEC TR 62681 has been prepared by IEC technical committee 115: High Voltage Direct Current (HVDC) transmission for DC voltages above 100 kV. It is a Technical Report.

This second edition cancels and replaces the first edition, published in 2014. This edition constitutes a technical revision.

This edition includes the following significant technical changes with respect to the previous edition:

a) the limits of total electric field in some countries have been supplemented and improved;
b) the definition of 80 %/80 % criteria of radio interference has been clarified;
c) a table has been added for bipolar excitation which shows the parameters of the IREQ radio interference excitation function;
d) the clause of CEPRI research results of audible noise has been deleted;
e) the clause of main conclusion of audible noise has been deleted.

The text of this Technical Report is based on the following documents:

Draft	Report on voting
115/289/DTR	115/292/RVDTR

Full information on the voting for its approval can be found in the report on voting indicated in the above table.

The language used for the development of this Technical Report is English.

This document was drafted in accordance with ISO/IEC Directives, Part 2, and developed in accordance with ISO/IEC Directives, Part 1 and ISO/IEC Directives, IEC Supplement, available at www.iec.ch/members_experts/refdocs. The main document types developed by IEC are described in greater detail at www.iec.ch/publications.

The committee has decided that the contents of this document will remain unchanged until the stability date indicated on the IEC website under webstore.iec.ch in the data related to the specific document. At this date, the document will be

- reconfirmed,
- withdrawn,
- replaced by a revised edition, or
- amended.

IMPORTANT – The "colour inside" logo on the cover page of this publication indicates that it contains colours which are considered to be useful for the correct understanding of its contents. Users should therefore print this publication using a colour printer.

INTRODUCTION

Electric fields and magnetic fields are produced in the vicinity of a High Voltage Direct Current (HVDC) overhead transmission line. When the electric field at the conductor surface exceeds a critical value, known as the corona onset gradient, positive or negative free charges leave the conductor and interact with the surrounding air and ionization takes place in the layer of surrounding air, leading to the formation of corona discharges. The corona discharge will result in corona loss but also change the electro-magnetic properties around the HVDC overhead transmission lines.

The parameters used to describe the electromagnetic performance of an HVDC overhead transmission line mainly include the:

1) electric field,
2) ion current,
3) magnetic field,
4) radio interference,
5) audible noise.

To control these parameters in a reasonable and acceptable range, for years, a great deal of theoretical and experimental research was conducted in many countries, and relevant national standards or enterprise standards were developed. This document collects and records the status of study and progress of electric fields, ion current, magnetic fields, radio interference, and audible noise of HVDC overhead transmission lines. It is recognised that general technical discussion given in this document would be applicable for HVDC sub-stations as well; However, since layout of a station differs very differently, expressions given for HVDC overhead transmission line cannot be directly used as many assumptions would not hold good. Furthermore, an HVDC sub-station is not accessible to the general public, thus the numbers and limits given in this document are not applicable for HVDC sub-stations.

ELECTROMAGNETIC PERFORMANCE OF HIGH VOLTAGE DIRECT CURRENT (HVDC) OVERHEAD TRANSMISSION LINES

1 Scope

This document provides general guidance on the electromagnetic environment issues of HVDC overhead transmission lines. It concerns the major parameters adopted to describe the electromagnetic properties of an HVDC overhead transmission line, including electric fields, ion current, magnetic fields, radio interference, and audible noise generated as a consequence of such effects. If the evaluation method and/or criteria of electromagnetic properties are not yet regulated, engineers in different countries can refer to this document to:

– support/guide the electromagnetic design of HVDC overhead transmission lines,
– limit the influence on the environment within acceptable ranges, and
– optimize engineering costs.

2 Normative references

There are no normative references in this document.

3 Terms and definitions

For the purposes of this document, the following terms and definitions apply.

ISO and IEC maintain terminological databases for use in standardization at the following addresses:

- IEC Electropedia: available at http://www.electropedia.org/
- ISO Online browsing platform: available at http://www.iso.org/obp

3.1
corona
set of partial discharges in a gas, immediately adjacent to an uninsulated or lightly insulated conductor which creates a highly divergent field remote from other conductors

[SOURCE: IEC 60050-212:2010, 212-11-44, modified – Note 1 has been deleted.]

3.2
electric field
constituent of an electromagnetic field which is characterized by the electric field strength E together with the electric flux density D

Note 1 to entry: In the context of HVDC transmission lines, the electric field is affected not only by the geometry of the line and the potential of the conductor, but also by the space charge generated as a result of corona; consequently, electric field distribution may vary non-linearly with the line potential.

[SOURCE: IEC 60050-121:1998, 121-11-67, modified – The original note has been deleted and Note 1 to entry has been added.]

3.3
space-charge-free electric field
electric field due to a system of energized electrodes, excluding the effect of space charge present in the inter-electrode space

3.4
ion current
flow of electric charge resulting from the motion of ions

3.5
magnetic field
constituent of an electromagnetic field which is characterized by the magnetic field strength H together with the magnetic flux density B

[SOURCE: IEC 60050-121:1998, 121-11-69, modified – Note 1 has been deleted.]

3.6
audible noise
unwanted sound with frequency range from 20 Hz to 20 kHz

[SOURCE: IEC 61973:2012, 3.1.14]

4 Electric field and ion current

4.1 Description of the physical phenomena

Electric fields are produced in the vicinity of an HVDC transmission line, with the highest electric fields existing at the surface of the conductor. When the electric field at the conductor surface exceeds a critical value, the air in the vicinity of the conductor becomes ionized, forming a corona discharge. Ions of both polarities are formed, but ions of opposite polarity to the conductor potential are attracted back towards the conductor, while ions of the same polarity as the conductor are repelled away from the conductor. Space charges include air ions and charged aerosols. Under the action of an electric field, space charge will move directionally, and ion current will be formed. The physical phenomena of electric field and ion current are described in this Subclause 4.1.

The electric field and ion current in the vicinity of an HVDC transmission line are defined mainly by the operating voltage, line configuration, conductor radius and conductor surface. The voltage applied to line conductors produces an electric field distribution. Unlike High-Voltage Alternating Current (HVAC) transmission lines, the electric field produced by HVDC transmission lines does not vary with time and, consequently, does not produce any significant currents in humans or objects immersed in these fields.

The electric field is another aspect of the electrical property around an overhead HVDC transmission line. An electric field is present around any charged conductor, irrespective of whether corona discharge is taking place. However, the space charge created by corona discharge under DC conditions modifies the distribution of an electric field. The effect of space charge on electric fields is significant.

For the same HVDC transmission lines, the corona onset gradients of positive or negative polarities are different and the intensity and characteristics of corona discharges on positive or negative conductors are also different. Consequently, during the design of HVDC transmission lines, special consideration needs to be paid to the allowable values of the maximum ground-level electric field and ion current density [1][1].

1 Numbers in square brackets refer to the bibliography.

Corona on a conductor of either positive or negative polarity produces ions of either the positive or negative polarities in a thin layer of air surrounding each conductor [1]. However, ions with a polarity opposite to that of the conductor are drawn to it and are neutralized on contact. Thus, a positive conductor in corona acts as a source of positive ions and vice-versa. For a monopolar DC transmission line, ions having the same polarity as the conductor voltage fill the entire inter-electrode space between the conductors and ground. For a bipolar DC transmission line, the ions generated on the conductors of each polarity are subject to an electric field driven drift motion either towards the conductor of opposite polarity or towards the ground plane, as shown in Figure 1. The influence of wind or the formation of charged aerosols are not considered at this stage. Three general space charge regions are created in this case:

a) a positive monopolar region between the positive conductor and ground,

b) a negative monopolar region between the negative conductor and ground,

c) a bipolar region between the positive and negative conductors.

For practical bipolar HVDC lines, most of the ions are directed toward the opposite polarity conductor, but a significant fraction is also directed toward the ground. The ion drift velocity is such that it will take at least a few seconds for them to reach ground. Actually, the molecules travelling along ion paths are not always the same ions. In fact, collisions between ions and air molecules occur during the travel at a rate of billions per second and cause charge transfer and reactions between ions and neutral molecules, so the ions reaching the ground are quite different from those that were originally formed by corona near the conductor surface. The exact chemical identity of the ions, after a few seconds, will depend on the chemical composition and trace gases at the location.

Electric field is another component of the electrical property around an overhead HVDC transmission line. Electric field is caused by electrical charges, both those residing on conductive surfaces (the transmission line conductors, the ground, and conducting objects) and the space charges. The effect of space charge on electric field is significant.

A nonlinear interaction takes place between electric field and space charge distributions in all three general space regions identified above in a), b), c). The nonlinearity arises because ions flow from each conductor to ground or to the conductor of opposite polarity along the flux lines of the electric field distribution: while at the same time, the electric field distribution is influenced by the ionic space charge distribution. In addition to the nonlinear interaction described above, the space charge field in the bipolar region is affected by other factors. Mixing of ions of both polarities in the bipolar region leads firstly to a reduction in the net space charge density and, secondly, to recombination and neutralization of ions of both polarities.

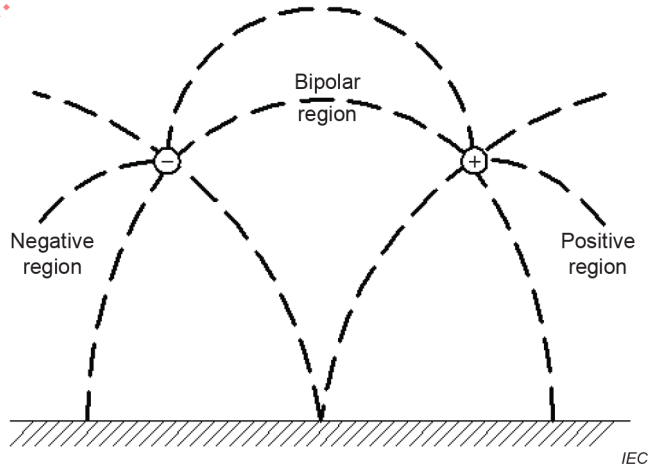

Figure 1 – Monopolar and bipolar space charge regions of an HVDC transmission line [1]

The corona-generated space charge, being of the same polarity as the conductor, produces a screening effect on the conductor by lowering the electric field in the vicinity of the conductor surface and consequently reducing the intensity of corona discharges occurring on the conductor. In the monopolar regions, the space charge enhances the electric field at the ground surface. The extent of electric field reduction at the conductor surface and field enhancement at the ground surface depend on the conductor voltage as well as on the corona intensity at the conductor surface. In the case of the bipolar region, however, the mixture of ions of opposite polarity and ion recombination tend to reduce the screening effect on the conductor surface. This leads to a smaller reduction in the intensity of corona activity near the conductors than in the monopolar regions.

The electrical environment at ground level under a bipolar HVDC transmission line is, therefore defined mainly by three quantities:

1) electric field, E,
2) ion current density, J,
3) space charge density, ρ.

The electric field produced by HVDC overhead transmission lines is a vector defined by its components along three orthogonal axes. The space charge density is a scalar. The ion current density is also a vector, and it is affected by the electric field and space charge density.

Very small currents in some cases can flow through an object or person located under the line because of exposure to the electric field and ion space charge. From the point of view of environmental impact on persons and objects located under the line, the main consideration is the combined exposure to the electric fields and ion currents. The scientific literature indicates that exposure to the levels of DC electric field and ion current density existing under operating HVDC transmission lines poses no risk to public health, but may cause some induced current and annoyance effects to humans.

Design of HVDC transmission lines requires the ability to predict ground-level electric field and ion current distribution as functions of line design parameters such as the number and diameter of sub-conductors in the bundle, height above ground of conductors and pole spacing. Prediction methods are based on a combination of analytical techniques to calculate the space charge fields and accurate long-term measurements under experimental as well as operating HVDC transmission lines.

As described and illustrated in Figure 1, the ground-level electric field and ion current property under a bipolar HVDC transmission line can be thought primarily as a monopolar space charge field under each pole. The bipolar space charge field between the positive and negative conductors, however, has no significant impact on the ground-level electrical property. For the purpose of calculating the ground-level electric field and ion current distributions, therefore, analytical treatment of the monopolar space charge field between each of the positive and negative conductors and the ground plane is adequate.

Monopolar DC space charge fields are defined by the following equations:

$$\nabla \cdot E = \frac{\rho}{\varepsilon_0} \tag{1}$$

$$J = \mu \rho E \tag{2}$$

$$\nabla \cdot J = 0 \tag{3}$$

where

E and J are the electric field and ion current density vectors at any point in space,

ρ is the space charge density,

μ is the ionic mobility,

ε_0 is the permittivity of free space.

The first Equation (1) is Poisson's equation, the second Equation (2) defines the relationship between the current density and electric field vectors, and the third Equation (3) is the continuity equation for ions. Since electrons are existent in the zone very close to the conductors and attached to air molecules forming negative ions, they are not considered. The solution of these equations, along with appropriate boundary conditions, for the conductor-ground-plane geometry of the HVDC transmission line, determines the ground-level electric field and ion current distributions [1].

Corona activity on conductors and the resulting space charge field are influenced, in addition to the line voltage and geometry, by ambient weather conditions such as temperature, pressure, humidity, precipitation and wind velocity as well as by the presence of any aerosols and atmospheric pollution. It is difficult, if not impossible, to take all these factors into account in any analytical treatment of space charge fields. Information on the corona onset gradients of conductors, which is an essential input in the analytical determination of electric field and ion current density, is also difficult to obtain under practical operating conditions. For these reasons, analytical methods are employed in combination with accurate long-term measurements of ground-level electric field and ion current distributions under experimental as well as operating HVDC transmission lines, in order to develop prediction methods. Some of the information required in the analytical treatment, such as corona onset gradients of conductors, can be obtained only through experimental studies. Reliable experimental data are also essential in validating the accuracy of analytical or semi-analytical methods for predicting the ground-level electric field and ion current distributions under HVDC transmission lines.

NOTE 1 Industry consensus and standards have not been reached on appropriate analytical methods to capture all effects of weather in the calculation of enhanced fields due to space charge.

NOTE 2 As described in reference [4], the conditions most conducive to enhanced fields due to space charge (wet conductor conditions in fog, with zero wind) occur for a very small percentage of time over a given year.

NOTE 3 As further pointed out in reference [4], to attempt to address very rare conditions in the design of an HVDC transmission line is not fully justifiable, given the lack of clear standards, analytical methods, and consensus on the subject.

The atmosphere has a large quantity of aerosol particles. When such particles are present in the ion flow around a stressed HVDC conductor, the ions will be captured by the particle because of Brownian motion and the motion driven by electric force. A charging process dictated by ions diffusing to particles is called diffusion charging [2]. This mechanism does not involve any external electric fields and some experiments indicate that it has insignificant relations with electrical properties of particles. Electrical properties are characterized by electrical conductivity and permittivity. As the charge accumulates on the particle surface, the electric field around the particle gets stronger, leading to a reduction of diffusion charging rate. The other charging process controlled by electric field is named field charging [2]. Unlike diffusion charging, several experiments show that the charging process relies heavily on the electrical parameters. The physical mechanism behind this phenomenon is Maxwell-Wagner relaxation of the electric field around the particle in the presence of an external electric field [3].

4.2 Calculation methods

4.2.1 General

Ground-level electric field and ion current distribution under HVDC transmission lines depend primarily on the conductor bundle and on the minimum height above ground of conductors. Pole spacing has a secondary influence on the electric field and ion current distributions, and is selected mainly on the basis of air gap clearances required to withstand the maximum values of overvoltage that can appear on the conductors.

Corona performance criteria, particularly for radio interference (RI) and audible noise (AN), are used to select the number and diameter of conductors in the bundle required on each pole. Conductor height and pole spacing have a secondary influence on the RI and AN performance.

Following the selection of the conductor bundle based on RI and AN design criteria, the minimum conductor height is selected on the basis of design criteria for ground-level electric field and ion current density. The conductor heights selected using these criteria are generally significantly higher than would be required from insulation and safety considerations.

Calculation of the desired ground-level electric field and ion current distribution for proposed HVDC transmission line configurations is, therefore, an essential step in selecting the minimum conductor height. Methods of calculation that are presently available for this purpose are described below.

Calculation methods for determining electric field and ion current distributions involve the solution of the boundary value problem described by the set of Equations (1) to (3) along with appropriate boundary conditions. The first rigorous analytical solution to the monopolar space charge modified field problem was obtained by Townsend [5] for the concentric cylindrical configuration. The main interest in this solution was to obtain the voltage-current characteristic for a thin wire at high voltage and in corona, placed concentrically inside a large metallic cylinder at ground potential.

Popkov [6] extended Townsend's solution to the geometry of a conductor above a ground plane and obtained a semi-empirical equation for determining the voltage-current characteristic. Popkov's solution is concerned mainly with the voltage-current characteristic and does not provide a solution for the ground-level electric field and ion current distribution.

Equations (1) to (3) define the monopolar corona problem for the general case of three dimensional electrode configurations. However, if the electrode geometry is characterized by symmetry in two dimensions, then the equations reduce to one dimensional form. For example, in the case of the concentric cylindrical geometry considered by Townsend, symmetry may be assumed to exist in the longitudinal and angular coordinates of the cylindrical coordinate system. The defining equations reduce, therefore, to one dimensional form in the radial coordinate, making it possible to obtain an analytical solution to the monopolar corona problem.

In the case of DC transmission lines, the geometry may be assumed to consist of a number of cylindrical conductors parallel to each other and also to the ground plane above which they are placed. This is essentially a two-dimensional geometry, since symmetry exists along the longitudinal direction of the conductors. The boundary value problem defined by Equations (1) to (3), therefore, reduces to a two-dimensional form in this case.

Since it is almost impossible to obtain analytical solutions to the two-dimensional space-charge-modified fields, such as those associated with DC transmission lines, it becomes necessary to use numerical techniques.

It should also be mentioned that the defining Equations (1) to (3) of monopolar corona do not take into account some of the practical considerations such as the influence of wind on the ion flow.

4.2.2 Semi-analytic method

The first method for solving Equations (1) to (3) for multiconductor DC transmission line configurations was developed by Maruvada and Janischewskyj [7] [8]. The method, originally developed to calculate corona loss currents, involves the complete solution of the monopolar space charge modified fields and, consequently, the determination of the ground-level electric field and ion current density distributions. The method of analysis does not include the influence of wind.

The method of analysis is based on the following assumptions:

a) the space charge affects only the magnitude and not the direction of the electric field,

b) for voltages above corona onset, the magnitude of the electric field at the surface of the conductor in corona remains constant at the onset value.

The first assumption, often referred to as Deutsch's [9] assumption, implies that the geometric pattern of the electric field distribution is unaffected by the presence of the space charge and that the flux lines are unchanged while the equipotential lines are shifted. Since HVDC transmission lines are generally designed to operate at conductor surface gradients which are only slightly above corona onset values, corona on the conductors generates low-density space charge and the ions may be assumed to flow along the flux lines of the space-charge-free electric field. This assumption is much more valid for DC transmission lines than for electrostatic precipitators where corona intensity and space charge densities are very high.

The second assumption, which was also implied in Townsend's analysis, has been justified from theoretical as well as experimental points of view [8].

In mathematical terms, the first assumption implies that:

$$E = \zeta E' \tag{4}$$

where

E is the electric field vector in the presence of space charge,

E' is the space-charge-free electric field vector,

ζ is a scalar point function which depends on the charge density distribution. The value of ζ at any point may be defined as the field modification factor.

This assumption has the distinct advantage of converting an essentially two dimensional problem into an equivalent one dimensional problem along the flux lines of the space-charge-free electric field. The boundary value problem defined by the partial differential Equations (1) to (3) are converted [8] to one described by the set of ordinary differential equations:

$$\frac{\mathrm{d}\Phi}{\mathrm{d}\varphi} = \zeta \tag{5}$$

$$\frac{\mathrm{d}\zeta}{\mathrm{d}\varphi} = -\frac{\rho}{\varepsilon_0 (E')^2} \tag{6}$$

$$\frac{\mathrm{d}\rho}{\mathrm{d}\varphi} = \frac{\rho^2}{\varepsilon_0 \zeta (E')^2} \tag{7}$$

where

E' and φ are the space-charge-free electric field intensity and potential respectively,

Φ is the potential in the presence of space charge,

ρ is the charge density,

ξ is the field modification factor, at any given point along the flux line.

The differential Equations (5) to (7) describe the variation of the dependent variables Φ, ξ and ρ as functions of the independent variables φ and E' along a flux line of the space-charge-free electric field. For a given line configuration and applied voltage, the flux lines of the space-charge-free electric field can be traced and values of E' and φ along any flux line determined [8].

The boundary conditions required to solve Equations (5) to (7) are given in terms of the voltage applied to the conductor and the magnitude of the electric field at the surface of the conductor in corona. If the voltage applied to the conductor with respect to the ground plane is U, the space-charge-free electric field at the conductor surface corresponding to the voltage U is E'_s, and the corona onset gradient of the conductor is E_0, then according to the second assumption, $\xi = \left(\frac{E_0}{E'_s}\right)$ at the conductor surface. The complete set of boundary conditions may then be written as

$$\Phi = U \text{ at } \varphi = U \tag{8}$$

$$\Phi = 0 \text{ at } \varphi = 0 \tag{9}$$

$$\xi = \left(\frac{E_0}{E'_s}\right) \text{ at } \varphi = U \tag{10}$$

If E'_g is the space-charge-free electric field at the point where the flux line meets the ground plane and ξ_g and ρ_g are the computed values at this point of the field modification factor and charge density respectively, the electric field E_g and ion current density j_g at this point are obtained as,

$$E_g = \xi_g E'_g \tag{11}$$

$$j_g = \mu \xi_g \rho_g E'_g \tag{12}$$

Where μ is the ion mobility.

The method developed by Maruvada and Janischewskyj can be applied to determine the ground-level electric field and ion current distributions under monopolar or bipolar DC transmission lines with single or bundled conductors and with or without overhead ground wires [8].

Application of the method developed by Maruvada and Janischewskyj requires knowledge of the geometric parameters of the line configuration, voltage applied to the line conductors and the corona onset gradients of the conductors. The calculation procedure requires the following steps:

1) for the given line configuration and conductor voltages, flux lines of the space-charge- free electric field, which originate on the conductors in corona and terminate on the ground plane, are traced;
2) for each flux line selected, the distribution of the electric field E' is determined as a function of φ along the flux line;
3) knowing the distribution of E' as a function of φ along the flux line, the boundary value problem defined by Equations (5) to (7) is solved, using the boundary conditions in Equations (8) to (10) to obtain Φ, ξ and ρ as functions of φ at all points along the flux line;
4) the magnitudes of the ground-level space charge modified electric field E_g and ion current density j_g at the point where the flux line terminates on the ground plane are then calculated using Equations (11) and (12);
5) by repeating steps 2 to 4 for a number of flux lines, the complete distributions of E_g and j_g along the ground plane are determined.

4.2.3 Finite element method

Gela and Janischewskyj [10] developed the first finite element method (FEM) for solving the monopolar space charge modified field problem without recourse to Deutsch's assumption. One of the main objectives of this study was to evaluate the errors which might result by the use of Deutsch's assumption in the Maruvada and Janischewskyj method.

The Gela and Janischewskyj method was developed specifically for the case of a monopolar DC line with a single conductor above ground [11] [12]. However, the method has the potential of further development for cases of lines with bundled conductors, overhead ground wires, etc.

For the FEM analysis, the defining Equations (1) to (3) of monopolar DC corona are expressed in terms of potential as,

$$-\nabla\cdot\nabla\Phi = \frac{\rho}{\varepsilon_0} \tag{13}$$

$$-\nabla\cdot(\rho\nabla\Phi) = 0 \tag{14}$$

$$\nabla\Phi = -\mathbf{E} \tag{15}$$

The set of Equations (13) to (15) is solved iteratively for Φ, by updating and recalculating the spatial distribution of ρ at the beginning of each iteration. The FEM [13] with linear triangular elements is employed to solve the partial differential Equations (13) and (15) for Φ at each iteration step. The iterative procedure is initiated with the first estimate obtained using the Maruvada and Janischewskyj method. Convergence of the iterative process is considered to have taken place when no further improvements are observed in ρ and both Equations (13) and (14) produce the same value of Φ.

Since Equations (13) and (14) are of second order, only two boundary conditions are needed to obtain a solution. These are provided by the values of Φ on the conductor surface and on the ground plane. The boundary condition that the magnitude of the electric field at the surface of the conductor in corona remains constant at the onset value, is not necessarily enforced during the solution of Equations (13) and (14). The extent to which this boundary condition is violated at any particular iteration provides information for updating and correcting the distribution of ρ for the next iteration, until convergence is achieved.

The final results of the iterative solution are values of ρ and Φ at the nodes of the finite element grid. Values of E, ρ and j at any points of interest, such as along the surface of the conductor or the ground plane, are derived subsequently.

Computational results obtained by the application of Gela and Janischewskyj method to the case of a monopolar DC line configuration with a single conductor lead to the following observations [12]:

a) distributions of electric field intensity at ground are not sensitive to Deutsch's assumption;

b) Deutsch's assumption can give rise to significant errors in the current density profiles at ground, particularly for certain line configurations operating at voltages well above corona onset;

c) however, for practical DC transmission line configurations and normal operating voltages, the use of Deutsch's assumption provides results of acceptable accuracy.

4.2.4 BPA method

A simplified method of analysis was developed at the Bonneville Power Administration (BPA) [14] for determining the ground-level electric field and current density under monopolar and bipolar DC transmission lines. In addition to the two assumptions mentioned in 4.2.2 and 4.2.3, other simplifying assumptions were made to develop the computer program ANYPOLE which was made available in the public domain. The other simplifying assumptions made in developing this program are:

– the conductor bundle is replaced by an equivalent single conductor with the same capacitance as the conductor bundle;

– the ion current is assumed to be uniformly distributed around a single conductor or an equivalent single conductor replacing the bundle.

Gaussian flux tube concept is used to obtain numerical solutions to the electric field and ion current distributions along the ground plane.

4.2.5 Empirical methods of EPRI

Empirical methods are generally derived from extensive experimental data obtained preferably on operating HVDC transmission lines, but also on full-scale test lines. In order to derive valid and accurate methods, the experimental data are obtained for lines of different voltages and configurations with a wide range of values for parameters such as conductor bundle, conductor height and pole spacing in the case of bipolar lines. The validity is usually restricted to the range of values of line parameters for which the experimental data, used to derive the empirical method, was obtained. Extrapolation of the empirical method outside the range of these parameters can give rise to significant errors.

Unfortunately, empirical methods based on good experimental data are presently not readily available for determining the ground-level electric field and ion current distributions under monopolar or bipolar DC lines.

A semi-empirical method, called the "degree of corona saturation" method, was proposed ([15], [16]) for calculating ground-level electric fields and ion currents under bipolar DC lines. This technique is incorporated in the workstation, an EPRI proprietary program. The basic principle of the method is given by the equation.

$$Q = Q_e + S\,(Q_S - Q_e) \tag{16}$$

where

Q_e is the electrostatic value of any parameter (electric field, ion current density or space charge density),

Q_S is the saturated value of the parameter

S is the degree of saturation.

The electrostatic value Q_e of the parameter can be calculated using the well-established electrostatic field theory. It should be noted that the electrostatic values of current density and charge density are zero.

Equations were derived for the saturated values of Q_S of the electric field, ion current density and charge density, based on laboratory tests on reduced-scale models with thin wires of monopolar and bipolar DC line configurations [17]. The degree of corona saturation factor S was derived from full-scale tests carried out on a number of bipolar DC line configurations.

It should be noted that the degree of corona saturation method is not a purely empirical method as described at the top of this Subclause 4.2.5. It involves some theoretical modelling and an assumption that results of scale model tests on thin wires can be extrapolated to the case of full-scale lines with practical conductor bundles. Questions were also raised on the difficulty in justifying some of the assumptions involved in the theoretical modelling from the point of view of basic corona physics.

4.2.6 Recent progress

Following the work of Gela and Janischewskyj, other FEM solutions were obtained for the space charge modified fields of both monopolar and bipolar DC transmission lines [18], [19]. In some of these studies, the solution was obtained assuming that the charge distribution on the conductor surface, rather than the electric field, was known and used as a boundary condition. Because of this assumption, these methods can be used to interpret experimental results but not for predicting the ground-level electric fields and ion current distributions for different transmission line designs with specified voltages applied to the conductors.

In other FEM based solutions [20] [21] [22] [23], the electric field boundary condition was used and, consequently, they can be used to predict the electric field and ion current distributions under practical DC transmission line configurations.

Using ion transit-time formalism, useful approximate calculations have been made [24] for space charge densities in a broad range of systems containing air ions.

In addition to those calculation methods mentioned in 4.2.2 to 4.2.5, the finite difference method [25], charge simulation method [20], multigrid method [26] and finite element method and finite volume method [27] are also used to predict the ground-level electric field under HVDC transmission lines.

4.3 Experimental data

4.3.1 General

In order to check the validity and accuracy of the calculation methods for ground-level electric field and ion current density distributions under HVDC transmission lines, it is necessary to compare the results of calculation with experimental data obtained on corona test lines and, preferably, on operating lines. The experimental data used in any comparison need to be measured using appropriate instrumentation and need to meet requirements of reliability and accuracy. It is also preferable to obtain long-term statistical data under different weather conditions. In addition to the electrical parameters required to characterize the electric field and space charge environment, the measurements need to include parameters defining the ambient weather conditions such as temperature, pressure, humidity, wind speed and direction and precipitation.

There may be uncertainties of measured values on electromagnetic fields from different laboratories and companies due to the use of different measuring techniques and instruments. This can lead to a difficulty in the measurement result interpretation and comparison. In this document, only the measurement results in different references are given, and the data are not evaluated.

4.3.2 Instrumentation and measurement methods

For both monopolar and bipolar DC lines, the electrical environment at ground level is characterized by the electric field intensity, ion current density and space charge density. In the case of bipolar DC lines, although ions of both polarities are created and mix in the bipolar region between the conductors, an essentially monopolar space charge of either positive or negative polarity exists at the ground level. In the presence of wind, the positive and negative ion profiles will shift and positive ions may drift toward the ground surface on the negative pole side of the DC line and vice-versa, depending on the direction of wind. The instrumentation and measurement methods for characterizing the electrical environment in the vicinity of DC lines are described in IEEE Std 1227 [28].

Different techniques have been used to measure the electric fields of HVDC over-head transmission lines, and basically two types of instruments are used to measure the electric field strength at ground level:

a) field mills;

b) vibrating plate electric field meters.

Both instruments measure the electric field strength by measuring modulated capacitively induced currents sensed by metal electrodes.

Field mills are commonly used to measure the electric field strength at ground level. A field mill instrument [29] consists essentially of a fixed sensing electrode above which a rotating shutter electrode is placed. As the sensing electrode is alternately exposed to and shielded from the electric field, a current is induced between the sensing electrode and ground that is proportional to the electric field strength. Measurement of the induced current, or voltage across known impedance that is located between the sensing electrode and ground, determines the electric field strength.

A vibrating plate instrument [30] consists of a sensing electrode placed below an aperture in a metallic plate and vibrated using a mechanical driver. The vibrations modulate charges induced in the sensor plate and the resulting current is proportional to the electric field strength. Measurement of the induced current, therefore, provides an indication of the electric field strength.

Ion current density at ground level is determined by measuring the current collected by a flat plate, known as a Wilson plate [31], located flush with the ground plane. The current density J, averaged over the area A of the plate, is given by:

$$J = \frac{I}{A} \tag{17}$$

Where I is the current collected by the plate.

Monopolar charge density is measured using aspirator-type ion counters [32]. The air ions are drawn through a parallel plate collector system using a motor driven blower. Alternate plates are connected together and a polarizing potential is applied between the two sets of plates. Collection of the ions on plates of opposite polarity gives rise to a current, which is measured using an electrometer. The charge density ρ measured by the ion counter is given as

$$\rho = \frac{I}{M_0} \tag{18}$$

where

I is the measured ion current

M_0 is the volumetric air flow rate.

Guidelines for the measurement of ground-level electric field strength, ion current density and space charge density under HVDC transmission lines are provided in the IEEE Std 1227 [28]. For accurate unperturbed measurement of these quantities the field meters, Wilson plates and ion counters are generally installed below ground so that the measuring interfaces of the instruments are flush with the ground plane. Significant errors may be caused in the measured quantities if these instruments protrude above the ground plane [28] unless values are corrected based upon measured form or correction factors for the altered geometry. The influence of a DC electric field on measurement of monopolar space charge densities with an ion counter can be made negligible when the measurements are performed in the ground plane, and oriented vertically or horizontally above the ground plane with an attractive potential applied to the ion counter housing. This assumes that the collecting electrode(s) in the ion counter is adequately shielded from the external electric field. The impact of rain and snow on the measurement instrumentation can also be considered during installation and use. Errors can result during rain or snow unless the instrumentation has been installed so that it can successfully operate during these conditions.

Because of large variations caused by weather conditions, long-term measurements are necessary to obtain statistical distributions as well as lateral profiles of the principal parameters. This is achieved by making simultaneous long-term measurements at several points in a plane perpendicular to the transmission line at mid-span [33], [34]. The measurement locations generally include points directly below the positive and negative conductors and at lateral distances of 15 m, 30 m and 60 m from the conductors on both sides of the line. More measuring points may be selected, depending on the availability of instruments, to obtain better lateral distributions.

If possible, the measurements need to be carried out at several locations along a line to take into account climatic differences that can occur at different locations on long HVDC lines. Climatic data at a number of points along the line can also be collected separately to establish the prevalence of conditions that could lead to increased field and ion current levels.

Calibration of the instruments is an essential part of the measurement program. A special parallel-plate apparatus [35], capable of generating known electric fields, ion current densities and space charge densities is required to calibrate all the instruments. Periodic calibration of the instruments, identification of possible sources of error and taking appropriate precautions [28] are necessary to ensure the validity and accuracy of the data acquired.

In addition to electric field strength, ion current density and monopolar space charge density, instruments have also been developed [28] for the measurement of electrical conductivity of air with a device known as Gerdien tube and the net space charge density using either a Faraday cage or a filter device. Conductivity measurements are rarely carried out under DC lines, but net space charge measurements are sometimes made at large distances from DC lines, mainly to detect the presence of charged aerosols.

4.3.3 Experimental results for electric field and ion current

Only a limited amount of experimental data are available in peer-reviewed publications on the corona performance of DC transmission lines, especially on operating lines and particularly on the ground-level electric field and ion current distributions. This may be attributed to a large extent to the technical difficulties and costs involved in making accurate and simultaneous long-term measurements at a number of points along a line perpendicular to the transmission line. Periodic calibration of the instruments is necessary to ensure acceptable accuracy of the long-term measurements.

Experimental data in peer-reviewed publications includes those obtained on outdoor test lines as well as operating HVDC transmission lines. However, test line data obtained at voltages well above the transmission voltages presently used and line dimensions (pole spacing and conductor height) outside the range used for practical line design [36] [37] are not included in this document. With this exclusion, the data available for possible comparison with any methods of calculation reduce to those obtained on four operating DC transmission lines [34] [38] [39] [40] [41] [42] and two test lines [43] [44]. Except for the BPA line [34], all other lines are located at approximately the sea level.

Details of line design parameters, adopted instrumentation and measurement program are described in the following. Statistical summaries of the experimental data obtained at each of the four test sites are also included.

For a bipolar horizontal line, the largest fields occur just outside each conductor. At all locations, the range of values of electric field depending on the variability of space charge. To describe the variable nature of electric field, the median and practical maximum are often given. The median level (L_{50}) is that exceeded 50 % of the time during the measurement period. Characterization of the practical maximum is also done in terms of an exceedance level, such as the L_5 exceedance level, i.e. the level exceeded only 5 % of the time.

The more and detailed experimental results for the electric field and ion current are shown in Annex A.

4.3.4 Discussion

The experimental data presented in 4.3.3, obtained on four operating DC transmission lines and three test lines, are probably the best data available in published literature. However, the database is not large enough to get significant conclusions regarding the influence of line parameters on ground-level electric field and ion current distributions.

The BPA ±500 kV DC line data are probably the best long-term data obtained in different weather conditions. The FURNAS ±600 kV DC line data was obtained during four one-month periods distributed over one year. The use of vibrating-plate field meters inverted and placed above a ground plane casts some doubt on the accuracy of electric field measurements in the presence of space charge in this study [28].

The test duration in the case of Manitoba Hydro ±450 kV DC line study is too short (four days). The short test duration and the use of single set of instruments for lateral profile measurements make it difficult to obtain an accurate statistical description of the data. Finally, the IREQ ±450 kV DC line data, although it is good from the aspect of test duration (one year) and instrumentation, were obtained on a test line rather than an operating line.

The BPA study has shown a significant asymmetry between the measured values of electric field and ion current density under the positive and negative poles of the line, with the levels under the negative pole being 2 to 3 times higher than those under the positive pole. This trend is also observed in the case of FURNAS line data, with the electric field and ion current levels under the negative pole being more than two times higher than those under the positive pole. No significant asymmetry has been observed, however, in the results obtained in the case of IREQ test line. Data at HVTRC have indicated asymmetry of field and ions for the polarities but vary by season. During the mid to late summer, the results under the positive pole were higher than those under the negative pole but opposite during the winter/very dry periods.

Electric field intensity and ion current density levels under BPA ±500 kV DC line were compared with calculations made using the BPA analytical method. It was found that the calculations agreed with the L_{10} levels of the measured probability distribution in fair weather conditions. It was also found that agreement between the calculated and measured levels was quite good for negative pole, but very poor for positive pole [186]. Similarly, a limited comparison was made between the measured lateral profile under the positive pole of the Manitoba Hydro DC line and calculations made using the Maruvada and Janischewskyj method [12]. It was found that calculations agreed well with measurements if a conductor surface irregularity factor of 0,4 was assumed.

Some new phenomena have been discovered in the test study in China and are shown as follows.

a) Effect of conductor pollution on the total electric field

   The previous pollution study is mainly about the effect on insulation level, and in the electromagnetic weather study, more attention is focused on rain, snow, and general pollution as by dust, smoke and insects. A test in the winter of 2007 [181] shows that the total electric field is larger when the conductor is dry and has been subject to pollution for a long period. After cleaning, the total electric field decreases greatly. The total electric field of clean conductor is almost half of that of a polluted conductor. So, it is necessary to study a quantitative description for pollution level and quantitative analysis for the effect of pollution on the total electric field.

b) Increase of the total electric field at ground with low humidity

   During the test in winter, it is discovered that the total electric field is obviously increased when the humidity is very low, but the current is almost the same [181]. There is no report about this phenomenon in domestic or international articles, and the mechanism needs to be studied in the future.

   Based on a review of published literature, it is concluded that the available experimental data on the electric field and ion current property under DC transmission lines is inadequate at present for purposes of rigorous comparison with existing methods of calculation or deriving any empirical methods of calculation.

4.4 Implication for human and nature

4.4.1 General

Static electric fields and space charge (i.e., air ions and charges on aerosols) are produced by DC transmission lines, but they are also generated by natural sources. This Subclause 4.4 summarizes scientific research on these electrical parameters in relation to humans and animals in nature. It also summarizes the conclusions of reviews prepared by scientific organizations and discusses applicable standards and guidelines.

4.4.2 Static electric field

Although static electric fields are present at varying levels in nature, relatively little biological research has been performed because the physical interaction of a static electric field with a human or animal body is confined to charges on the surface of the organism. No currents or electric fields are induced inside the body. At sufficiently high levels, a static electric field can be sensed by the movement of body hair [45] [46] [182].

A psychophysical study of the ability of human subjects under carefully controlled conditions to detect a static electric field reported a range of perception thresholds, but the average critical detection value was 40,1 kV/m; when air ions were present in high concentrations, the threshold was lower [47]. Testing conducted outdoors indicated that most people would not detect static electric fields at a level under 25 kV/m [48] [163]. It should be noted that the enhanced electric field under an HVDC line is not expected to be over 50 kV/m.

Other studies of human subjects exposed to static electric fields over a range of field strengths between 1 kV/m and 90 kV/m of varying duration, including daily exposures for up to 6 months, report no consistent behavioural or physiological responses (e.g. [49] [50] [51] [52]).

A variety of studies have also examined behavioural and biological responses of animals to static electric fields. Except for a few isolated reports of behavioural responses to high-strength static electric fields, these studies report no effects [183]. It should be noted that if the field could be detected by animals, this sensory stimulus could be expected to affect a range of spontaneous and trained behaviours.

Some of the most important studies in this group are those that looked for evidence of toxicity at longer durations of exposure. Fam found no adverse effects of long-term exposures of rats and their offspring to 340 kV/m static electric fields [53]. Kellogg and Yost reported no difference in the longevity of mice exposed to 2 kV/m static electric fields or ambient field conditions [54]. A laboratory at The Rockefeller University reported that exposure of rats to static electric fields of 3 kV/m and 12 kV/m for 2 h, 18 h, and 66 h had no effect on behaviour or brain neurotransmitter activity [55] [56] [57].

Under most circumstances, the static electric fields from a 500-kV DC transmission line would not be strong enough to be perceived, particularly outside the right-of-way (ROW). The absence of a mechanism by which static electric fields could produce an exposure to cells inside the body combined with the absence of human and animal evidence for adverse effects are important considerations in the assessment of potential effects. If a person (or large object) were to be very well insulated from the ground in a static electric field substantially greater than 25 kV/m, however, transient spark discharges to grounded objects could lead to annoying shocks, like a carpet shock in one's home.

4.4.3 Research on space charge

4.4.3.1 General

Since their discovery [58], air ions and charged aerosols have been studied for effects on humans and animals, as well as microorganisms, plants and insects. Within each of these species, there are few studies of substantial depth and quality and with findings that have been verified by other independent investigators. Most studies fail to control crucial aspects of the experimental situation that can significantly influence the outcome of the experiment.

For the purposes of this document, the focus will be limited to studies of humans and animals. Since exposures to air ions in nature and laboratories necessarily involve exposure to some charged aerosols, all studies reflect exposures to both forms of space charge to a greater or lesser extent.

As with static electric fields, the interaction of space charge with an organism is limited to the surface of the body with the exception that air ions and aerosols may attach to the interior of the respiratory tract during respiration. Given the potential for internal exposures from airborne ions and aerosols by respiration and the prevalence of media and scientific attention to potential behavioural and psychological effects of air ions, research on these two topics is the focus of the following discussion.

4.4.3.2 Air ions

The effects of artificially generated air ions on humans have been studied for both experimental and clinical therapeutic purposes. A wide range of concentrations has been tested on humans, but there is no good evidence that effects attributed to air ion exposure are more likely at higher ion concentrations.

Some experimental sources of air ions also produce excessive levels of ozone, an irritant gas, but few investigators have checked for or measured this potential source of inaccuracy. Measurements and calculations of ozone levels near DC transmission lines show that the amounts generated are small and disperse to levels that are barely measurable and, thus, have no health safety environment (HSE) consequence. Ion concentrations are generally lower than $1{,}0 \times 10^5$ ions/cm^3 at DC transmission lines in fair weather and lower than $2{,}0 \times 10^4$ ions/cm^3 at the edge of the right-of-way (ROW). Some examples of typical air ion concentrations (ions/cm^3) found at other locations are: (HSE can be defined)

- Fair weather open space $7{,}0 \times 10$ to $2{,}0 \times 10^3$ ions/cm^3
- In large towns up to $8{,}0 \times 10^4$ ions/cm^3
- 0,30 m (12 in) above burning match $2{,}0 \times 10^5$ to $3{,}0 \times 10^5$ ions/cm^3
- 60,96 m (200 ft) from small waterfall $1{,}5 \times 10^3$ to $2{,}0 \times 10^3$ ions/cm^3
- 1,52 m (5 ft) downwind of vehicle exhaust about $5{,}0 \times 10^4$ ions/cm^3

While some studies have suggested that positive ions may adversely affect pulmonary function [59] [60] [61] [62], other more systematic and quantitative experiments, as well as a double-blind clinical study, have not substantiated this suggestion [63] [64] [65] [66] [67] [184].

In some early studies, the investigators reported respiratory irritation. Respiratory dryness or irritation symptoms were reported in one of these early studies by about 20 % of subjects exposed to $5{,}0 \times 10^3$ ions/cm^3 to $1{,}0 \times 10^4$ ions/cm^3 [68]. The study, however, was blind (not double-blind) and was conducted during the winter, when upper respiratory symptoms are common, as pointed out by the study's author.

In a series of double-blind clinical studies [61], positive ions were more effective in producing irritation symptoms than negative ions at the lower exposure levels, but not at higher exposure levels (10^5 ions/cm^3). Symptoms were minor and included headache, nasal obstruction, husky voice and sore throat, itching nose, or dizziness in 16 subjects exposed to $3{,}2 \times 10^4$ positive ions/cm^3. Similar symptoms were experienced in 4 of 13 subjects exposed similarly to negative ions. Studies also have shown, however, that exposure to air ions did not result in respiratory irritation symptoms at exposure levels of $1{,}0 \times 10^4$ ions/cm^3 [65], $1{,}25 \times 10^5$ ions/cm^3 [64], and $5{,}0 \times 10^5$ ions/cm^3 [66].

Subjects with asthma, hay fever, or chronic obstructive pulmonary diseases seemed not to be at excess risk of irritation symptoms [61] [63].

Although some studies have suggested beneficial effects of short-term exposure to negative air ions for the treatment of allergies or asthma [59] [60] [64], other more rigorous studies have demonstrated that neither negative nor positive ions have a substantial effect on symptoms of asthma or hay fever, an effect on response to allergens or irritants at the transmission lines, or an effect on histamine sensitivity in the asthmatic [63] [65] [67] [69] [70].

Evidence of an effect of air ions on either short- or long-term lower respiratory diseases is lacking. Air ions or their reaction products, however, are reported to affect sputum production or viscosity in short-term lower respiratory diseases [62] [66]. More recent studies of rats exposed to $3{,}5 \times 10^5$ ions/cm^3 suggest that exposure activated goblet cells without producing damage to the trachea [71].

As with the human studies, exposures of rats or mice to air ions are not reported to cause clear or consistent effects. These include studies of respiration rates at ion levels greater than $3{,}0 \times 10^5$ ions/cm^3 [72] [73]. Life-long exposures of mice (about 2 years) reportedly reduced the longevity of mice exposed to negative ions ($2{,}0 \times 10^3$ ions/cm^3 or $2{,}0 \times 10^5$ ions/cm^3) compared to mice in the grounded control or groups exposed to positive ions [54]. The data were internally inconsistent and there was no apparent dose-response relationship. The authors acknowledge in an earlier report of data from the study that a vitamin deficiency in the mice and "the prevalence of proteus infections markedly complicates the interpretation of the cause of death for affected experimental animals" [74].

Studies in which mice were exposed to influenza virus, pneumonia, or C. immitis fungus and air ions showed no consistent relationship between exposure level or ion polarity and outcome at levels of $1{,}0 \times 10^4$ to $5{,}0 \times 10^5$ ions/cm^3 [75] [76] [77] [78] [79]. In these latter studies, differences between exposed and unexposed animals were not greater at higher exposure levels nor was there consistency as to effects of ions of either polarity. In the longest series of experiments from Krueger's laboratory, there was no explanation for the failures to replicate effects despite the similarity of exposures and other conditions [76] [77] [78] [79].

Studies of air ions have been conducted more frequently on psychological and behavioural parameters than on physiological parameters. One reason was the nationwide publicity given to anecdotal claims in several American national magazines in the 1960s that artificially generated negative air ions would improve mood and feelings of wellbeing while positive ions would increase subjective complaints. To this date, such notions have generated much popular interest but little scientific support. The relevant research is summarized below.

A variety of studies have examined the effects of positive and negative ions on indicators of human behavioural states, which could be considered to be indicative in some way of mood. The better studies were carried out in a controlled fashion. Of these controlled studies, some report no effect of positive or negative ions on mood (McGurk et al. at $8{,}0 \times 10^4$ ions/cm^3 [80], Chiles et al. At $2{,}6 \times 10^4$ ions/cm^3 [81], Finnegan et al. at 1 841 ions/cm^3 [82], Hedge and Collins at $2{,}0 \times 10^4$ ions/cm^3) [83], while others reported an effect as discussed below.

Hawkins et al. reports that a 3-week exposure to negative ions at $2{,}7 \times 10^4$ ions/cm^3 improves the ratings of health relating comfort, but the responses were not consistent across shifts or work areas [84]. The differences in subject ratings between exposed and unexposed time periods were smaller than those produced by temperature and humidity alone.

Charry and Hawkinshire report exposure for 1,5 h between $2{,}0 \times 10^4$ ions/cm^3 and $3{,}0 \times 10^4$ ions/cm^3 lowered indices of sociability and increased tension [85].

Siegel reported that exposure to both positive and negative ions at $1{,}0 \times 10^5$ ions/cm^3 had no effects on five of seven mood indicators, but indicators of vigour and friendliness were enhanced with exposure to air ions of either polarity [86].

Several studies have looked for therapeutic effects of air ion exposure on the mood of patients with depression related to seasonal affective disorder. A reduction in depressive symptoms was recorded for patients exposed to $2{,}7 \times 10^6$ ions/cm^3 but not those exposed to $1{,}0 \times 10^4$ ions/cm^3 [87], a finding also reported in later studies [88] [89]. Perez et al. reports that negative air ionization is associated with lower depression scores particularly at the highest exposure level [185]. No adverse symptoms were attributed to exposure to air ions in any of these three studies. The mechanism for how air ions could have contributed to these results, however, is not clear. Simple sensory stimulation could be involved since the presentation of auditory stimuli, bright light, or high levels of air ions all were reported to reduce ratings of depression, mood disturbance, and anger within 13 min to 30 min [90].

An additional consideration is suggested by the Terman and Terman study in which the responses of subjects in all treatment groups (including air ions) were correlated significantly with pre-treatment expectations of potential benefit. These results raise the issue of placebo responses [88].

Several groups of investigators have hypothesized that behavioural, psychological, and respiratory responses of humans and animals to air ions are related to effects on the metabolism of the neurotransmitter, serotonin. A clinical physician in Israel suggested that increases in positive ion concentrations associated with hot dry weather conditions or higher levels generated artificially at $1{,}0 \times 10^5$ ions/cm^3 increased levels of serotonin and its metabolite in the blood and urine of patients. Negative ions were reported to reduce the levels of serotonin and its metabolite [91] [92] [93]. These studies are of limited value because of the poor experimental control over their conduct, including exposures and analysis [94] [95].

Krueger's laboratory conducted similar studies in mice and reported changes in the levels of serotonin in the blood of mice (see [96] for summary and review), but others have been unable to replicate this effect [74] [96]. The Krueger laboratory also reported changes in the concentration of serotonin in the brains of mice and rats exposed to levels between $4{,}5 \times 10^4$ ions/cm^3 and $5{,}0 \times 10^5$ ions/cm^3 for as little as 12 h or for as long as 20 days, but no effect on serotonin or its metabolite in the brains of rats exposed to $5{,}0 \times 10^5$ ions/cm^3 for 2 h, 18 h, or 66 h [57].

The quality of research studies on air ions is low because of the difficulty associated with characterization of exposures, the control of relevant physical factors, and other design and analysis issues. The data does not indicate an established response among humans or animals at air ion levels less than $1{,}0 \times 10^4$ ions/cm^3. At levels between $1{,}0 \times 10^4$ ions/cm^3 and $1{,}0 \times 10^5$ ions/cm^3, a wide variety of biological and behavioural responses have been investigated, but the studies in aggregate provide no reliable basis to conclude that such exposures influence biological responses. For responses that are reported, there are other studies that report contradictory findings. The expectation that larger or more reliable effects might be observed at still higher exposure levels, i.e. greater than $1{,}0 \times 10^5$ ions/cm^3, was not supported, but too few studies at levels above $1{,}0 \times 10^6$ ions/cm^3 have been performed to characterize responses to extremely high levels.

4.4.3.3 Charged aerosols

In the 1930s and the 1940s, investigators in Germany experimented with electrified water droplets and other aerosols used in the treatment of a variety of respiratory conditions. These exposures produced a very large number of charges per particle. While there were anecdotal reports of relief of symptoms, apparently no double-blind studies were performed to confirm any beneficial effects [97]. Such exposures to highly charged aerosols would be expected to increase their deposition in the respiratory tract as predicted by Wilson [98].

Fraser reported that a large number of charges (> 1 000) per particle were necessary to produce a 2-fold increase in the deposition of particles in the respiratory tract of rabbits [99]. Melandri et al. reported that 30 to 110 charges/particle were required to increase the deposition of small particles (0,3 µm to 1,1 µm) in human subjects by 13 % to 30 % [100].

Researchers at a physics research laboratory at Bristol University have hypothesized that corona on AC transmission lines causes electrical charges to attach to particles so as to enhance their retention in the respiratory tract and can affect health by increasing exposure to ambient pollutants [101] [102].

There has been no empirical demonstration that the levels of charge on aerosols under this hypothesis, however, would be sufficient to enhance deposition of aerosols. This hypothesis has been criticized on the grounds of physical modelling [103] [104]. Jeffers reported that modelling and analyses of power lines and air ionizers indicate that particles are unlikely to become sufficiently charged to increase deposition within the respiratory tract [104]. This topic was investigated by an independent group of scientists for the NRPB, who concluded that charged ions (corona ions) were not likely to contribute to significant health effects [48].

This hypothesis could also be applied to DC transmission lines. Johnson has made direct measurements of the charge on aerosols by size downwind from a monopolar DC transmission line [16] [106] [107]. In ambient conditions of roughly equal numbers of negative and positive small air ions (600 ions/cm^3 to 800 ions/cm^3), the net average number of charged aerosols was zero. The number of charges on individual aerosols, however, varied from several negative to several positive charges for these conditions. When the DC transmission line was in heavy corona, the charged aerosol levels were generally 10 000 charges/cm^3 or less at ground level near the line (within 30 m or 100 ft) and had only single digit charge states. Even when the charge distribution was shifted by the ions produced by the DC transmission line, some of the aerosols still retained charge opposite to the polarity of the DC transmission line.

4.4.3.4 Studies of DC transmission lines

Studies also have been performed on the health and behaviour of humans and animals living near or under DC transmission lines. An effect of ion current is the charging of objects. The voltage that the object acquires depends on the magnitude of the ion current and on the impedance between object and ground. If a person touches the object, the person may discharge it through a spark. However, such sparks occur infrequently because most objects do not accumulate enough charge.

Haupt and Nolfi reported on a home survey of 438 respondents in 128 households in an exposed and a control suburb along the Pacific Intertie, a transmission line then operated at ±400 kV [108]. No differences in short-term symptoms or overall health were found between the two groups. Exposures were estimated by distance alone; the investigators assumed for the purposes of the analysis that residents living within about 0,22 km (0,14 miles) of the line were exposed and those living 1,04 km to 1,36 km (0,63 miles to 0,85 miles) distant were not exposed. Although the data were well-collected and the analyses conducted carefully and perceptively, the report is not technically robust and, therefore, has limited value. Other limitations have been discussed in a letter to the editor [109].

An epidemiology study of the performance and reproduction of over 500 herds of dairy cows near a ±400kV DC transmission line in Minnesota was performed for the Minnesota Environmental Quality Board (MEQB) [110]. Data on approximately 24 000 milking cows, including average daily milk production, percent of animals that experienced high and very high drops in milk production, and annual average herd milk production in first and third lactations, were compared across six categories of distance ranging from 0 miles to 1/4 mile or 0,4 km (stratum 1) out to 6 miles to 10 miles or 9,6 km to 16 km (stratum 6) and time periods before and after energization of the line in 1979. Similarly, data on reproduction, including inter-calving intervals, abortions, infertility-related culling, and mortality, were analyzed. No differences were reported in any of these variables before or after energization or as a function of distance from the transmission line. The strengths of this study include the very large number of cows studied and the very sensitive, if non-specific, indicators of adverse effects.

Investigators at Oregon State University compared the health and productivity of 200 cow-calf pairs randomly assigned to pens directly under or 615 m away from the Pacific Intertie ±500 kV DC transmission line. No differences between the animals in the exposed and control pens were noted with regard to breeding activity, conception rate, calving, calving interval, body mass of calves at birth, body mass at weaning, or mortality over a 3-year period. The average exposure of the animals in pens under the line was about 5 kV/m and 13,000 ions/cm^3 [111].

As part of this study, the investigators also monitored the activities of the exposed and control cattle at 13 min intervals during a 24 h period each month [112]. The distribution of cattle along feed troughs in the exposed and control pens was similar and unrelated to measures of the static electric field and there were no major differences in the time spent in various behaviours. Although small differences in the distribution of cattle within the pens were noted, the investigators reported that the differences were not correlated with fluctuations in the static electric field or noise levels.

In China, in combined AC and DC electric fields under AC and DC test line sections in the same corridor, a large number of tests have been carried out to investigate the sensitivity of human subjects. The tests have investigated the effects of both insulated human bodies touching earthed metal objects, and earthed human bodies touching insulated metal objects [187].

4.4.4 Scientific review

4.4.4.1 General

Over the last 30 years, health agencies have convened groups of scientists to review biological research on exposures to static electric fields and air ions. These groups assembled by the MEQB, the International Agency for Research on Cancer (IARC), the Health Protection Agency of Great Britain (HPA), and the World Health Organization (WHO) have included dozens of scientists with diverse skills that reflect the different research approaches required to answer questions about health. These scientists evaluated the strengths and weaknesses of individual studies in the literature and then evaluated all of the research together to determine what effects of exposures, if any, might be expected at different levels of exposure, i.e., a comprehensive weight-of-evidence review. These weight-of-evidence reviews and their conclusions are summarized below.

4.4.4.2 Minnesota environmental quality board

In 1981, the MEQB convened a expert panel of seven scientists to evaluate the health and safety aspects of a recently constructed ±400 kV transmission line in Minnesota to determine if permits for the line protected public health and safety and what, if any, additional standards were necessary to protect public health [113]. Their review continued over several years and the majority report concluded that air ions are not well established as a cause for biological effects, and even if these effects were to be substantiated, they posed no hazard to human or animal health. The science advisors later evaluated additional research and monitoring data and again concluded that there was little likelihood that either chronic or acute exposure to small air ions and static electric fields at levels measured either on or downwind of the ROW of the DC transmission line would cause adverse health effects [114].

4.4.4.3 International Agency for Research on Cancer (IARC)

The primary mission of the IARC is to coordinate and conduct research on the causes of human cancer, the mechanisms of carcinogenesis, and to develop scientific strategies for cancer prevention and control. The best-known activity of the IARC is the preparation of reviews of technical physical factors (i.e. IARC Monographs) to assess the possibility that they can increase the risk of human cancer. IARC's Monographs have included assessments of chemicals, complex mixtures, occupational exposures, physical and biological agents, and lifestyle factors. National health agencies use this information as scientific support for their actions to prevent exposure to potential carcinogens.

Interdisciplinary working groups of expert scientists are convened by the IARC to review the published studies and evaluate the weight of evidence that an agent can increase the risk of cancer. Their reviews are performed according to scientific principles, procedures, and criteria. Since 1971, more than 900 agents have been evaluated.

An IARC Task Group reviewed scientific research on static electric fields as part of a larger study of AC fields [115]. For static electric fields, the task group concluded that there is inadequate evidence of carcinogenicity in humans, and no relevant data were available from studies of experimental animals. Therefore, static electric fields were judged not classifiable as to their potential carcinogenicity in humans.

4.4.4.4 Health protection agency of the United Kingdom

The former National Radiological Protection Board (NRPB) had a long history of providing support and advice to the National Health Service, the Department of Health, and other government bodies in the United Kingdom on public health issues relating to ionizing radiation and electromagnetic fields. The NRPB has issued reviews and assessments on static electric fields and charged aerosols.

In 2004, the NRPB published a review of epidemiologic and biological studies and physical mechanisms of interactions of static electric fields [48]. The NRPB concluded that the most robust response to static electric fields was cutaneous perception. The threshold for perception was reported around 20 kV/m and annoying sensations were induced above 25 kV/m. The NRPB agreed with the IARC [115] that overall, the effects of static electric fields in humans do not suggest that exposure is associated with significant health effects.

The NRPB also has reviewed research on air ions and charged aerosol particles. A group of scientists was assembled to provide input to the Advisory Group on Non-Ionising Radiation (AGNIR) of the NRPB on the possible effects of corona ions of static electric fields on exposure to airborne pollutants and address the question whether corona ions increase the dose of relevant pollutants to target tissues in the body [48]. The conclusion of AGNIR was that "the additional charges on particles downwind of power lines could also lead to deposition on exposed skin. However, any increase in deposition is likely to be much smaller than increases caused by wind." Their conclusion identified uncertainties about the inhalation of charged particles, but stated, "However, it seems unlikely that corona ions would have more than a small effect on the long-term health risks associated with particulate pollutants, even in the individuals who are most affected" [48]. This assessment has been reaffirmed by the WHO in 2007 [116].

4.4.4.5 World Health Organization

The WHO is the division of the United Nations that is responsible for providing leadership on global health matters, shaping the health research agenda, setting norms and standards, articulating evidence-based policy options, providing technical support to countries, and monitoring and assessing health trends.

Of these four scientific agencies indicated, the WHO conducted the most recent assessment of static electric fields in 2007 [116]. An important consideration in the WHO's assessment was that a static electric field does not penetrate electrically conductive objects such as the human body; the field only induces a surface electric charge. Thus, the potential for effects on the body are limited to those related to the perception of the density of charge on the surface of the body by its interaction with body hair and by other effects such as spark discharges (micro shocks). At sufficiently high levels, this perception can produce annoyance and discomfort.

Overall, the WHO review also supported the conclusions of the IARC [115] that static electric fields could not be classified as to their potential relevance to cancer processes. The WHO made no recommendations for further research concerning biological effects from exposure to static electric fields or the need for any human epidemiology studies.

None of the scientific weight-of-evidence reviews conducted to date concluded that any adverse health effects of exposure are likely, but micro shocks under some conditions under a DC transmission line could be annoying or cause a shock.

4.5 Design practice of different countries

The electric field and ion current limits at ground level are the important foundations for the determinations of conductor patterns and line configurations, and reasonable limits are important for health and safety protection and project cost control.

At the initial stage of UHVDC project studies in China, the electromagnetic properties of UHV project is controlled to be not more than the level of the electromagnetic properties of EHV project. Based on the analysis and studies of national and international electromagnetic limits of DC and AC lines, combining the actual situation in China, after the test, calculation, and analysis for the technical feasibility and economy, the electric field and ion current limits for ±800 kV DC lines in China have been put forward and shown in Table 1.

Table 1 – Electric field and ion current limits of ±800 kV DC lines in China

Electromagnetic HSE parameters	Limits
Electric field (kV/m)	30 (under lines, on the ground) 15 (residential areas (nearby residential housing), wet conductors, on the ground)
Current density (nA/m^2)	100 (under lines, on the ground)

The electric field and ion current limits for DC lines in the United States of America, Canada and Brazil are respectively shown in Table 2 to Table 4.

Table 2 – Electric field limits of DC lines in United States of America [121]

Department	Limits
Department of Energy (kV/m)	30 (under lines, on the ground) 15 (space charge free electric field (static electric field), on the ground)
North Dakota State (kV/m)	33 (under lines, on the ground)
Minnesota State (kV/m)	12 (space charge free electric field (static electric field), on the ground)

Table 3 – Electric field and ion current limits of DC lines in Canada

Electromagnetic HSE parameters	Limits
Electric field (kV/m)	25 (under lines, on the ground)
Ion current density (nA/m^2)	100 (under lines, on the ground)

Table 4 – Electric field limits of DC lines in Brazil

Electromagnetic HSE parameters	Limits
Electric field (kV/m)	40 (under lines, on the ground) 10 (at the edge of the RoW,on the ground)
Ion current density (nA/m^2)	100 (under lines, on the ground) 5 (at the edge of the RoW,on the ground)

5 Magnetic field

5.1 Description of physical phenomena

The DC magnetic field is produced by the current in the conductors of an HVDC transmission line, and the magnetic field is also a parameter of the electromagnetic property of an HVDC transmission line. The description of the physical phenomena of magnetic field is given in this Clause 5.

The DC magnetic field produced by an HVDC transmission line does not vary with time, and it is different from the AC magnetic field produced by a HVAC transmission lines. Unlike the electric field under an HVDC transmission line, if there are no existing magnetic substances in the vicinity of an HVDC transmission line, the DC magnetic field will not be deformed generally. The DC magnetic field is defined mainly by the operating current and the line configuration, and its magnitude is in proportion to the magnitude of the current in the conductors and falls off rapidly away from the conductors.

The magnetic induction intensity is usually used to describe the magnetic field of a DC transmission line. For AC transmission line, the image conductor needs to be considered when its magnetic field is calculated. The equivalent depth of image conductor is defined by the Equation (19):

$$d = 660\sqrt{\frac{\rho}{f}}(m) \tag{19}$$

where

ρ is the resistivity of the earth;

f is the frequency.

For the DC current, f is equal to zero and the equivalent depth of image conductor can be thought of as infinite, so only the magnetic field produced by the current of conductors above the ground need be calculated.

If DC transmission line is considered to be infinite and straight, Ampere's circulation theorem can be used to calculate its magnetic field. The actual DC transmission line is not infinite and straight, so Biot-Savart's law can be adopted to calculate its magnetic field by integrating.

5.2 Magnetic field of HVDC transmission lines

In some countries, such as China, the impact on the instruments of geomagnetic observatory needs to be considered during the design of DC transmission lines, and a minimum distance between geomagnetic observatory and the DC lines needs to be specified. The International Commission on Non-Ionizing Radiation Protection (ICNIRP) gives the suggested limit of general public exposure to static magnetic fields as 400 mT. German regulations give a limit of 500 uT for DC magnetic field for general public. China, Poland, the Netherlands and Switzerland also have limits below ICNIRP suggestion of 400 mT. Even in the corridor of HVDC lines, magnetic field from HVDC lines is about the same as the geomagnetic field and markedly decreases with distance from HVDC lines. Figure 2 indicates the lateral profile of magnetic field of a Chinese ±800 kV HVDC line whose operating current is 4 000 A, under the bipolar operation condition. The clearance between positive polarity and negative polarity is 22 m. Curves from top to bottom represent line height from 17 m to 25 m. Even at the lowest height of HVDC line (18 m), the maximum magnetic field at ground level is less than 45 μT, whereas the geomagnetic field in most areas of the world is 20 μT to 70 μT. It is obvious that the maximum magnetic field of a ±800 kV HVDC line on the ground surface, under rated current operating conditions, is on the same level as the geomagnetic field experienced in most parts of the world. Thus, magnetic limit is not a design consideration for HVDC lines.

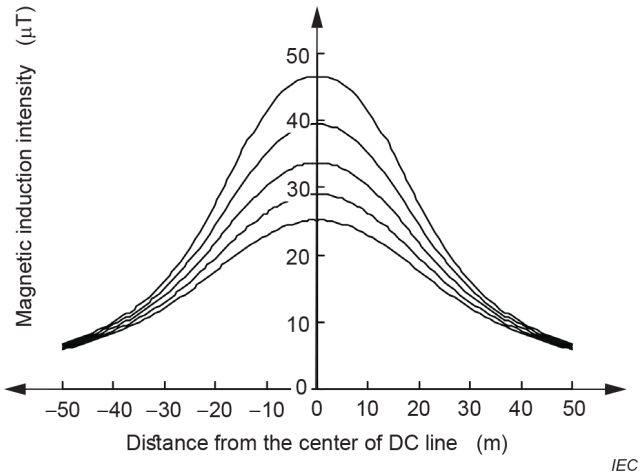

Figure 2 – Lateral profile of magnetic field on the ground of ±800 kV HVDC lines

6 Radio interference

6.1 Description of radio interference phenomena of HVDC transmission system

6.1.1 General

Radio interference (RI) generated from the HVDC transmission systems is caused in two ways: firstly, by normal operation of the main converter valves; secondly, by corona discharge and associated phenomena on high voltage equipment, bus bars and overhead lines. The corona in the converter stations can affect a long distance along the transmission lines, such as 10 km. The following discussion is about those sections of the HVDC lines far from the converter stations, where the impact of HVDC converter valves is insignificant.

Radio interference from the HVDC overhead power lines can be generated over a wide band of frequencies by [120]:

a) corona discharges in air at the surfaces of conductors and fittings;

b) discharges and sparking at highly stressed areas of insulators;

c) sparking at loose or imperfect contacts.

The sources of a) and b) are usually distributed along the length of the line, but source c) is usually local. For lines operating at voltages above 100 kV, the electric stress in air at the surface of conductors and fittings can cause corona discharges. Sparking at bad contacts or broken or cracked insulators can give rise to local sources of radio interference. High voltage apparatus in converter stations can also generate radio interference which can be propagated along the overhead lines. However, this is strictly regulated by radio interference voltage tests at factory. This document focuses on radio interference phenomena due to corona discharge.

In the description of the empirical/predication formulas of this document, the information of the detector type is quasi-peak.

6.1.2 Physical aspects of DC corona

The physical aspects of the DC corona mechanism are different from those of AC corona, because:

a) a stationary ionization sheath is created around each conductor;

b) a space charge is built up in the remaining space between the conductors and ground and between conductors themselves.

Corona discharges are initiated by collisions of free electrons with stable atoms. These electrons exist in the atmosphere under all normal conditions and move away from the negative conductor towards the positive conductor. This leads to a significant difference between the two resulting forms of corona. Negative corona discharges occur at a high repetition frequency and moderate amplitude, whilst those near the positive conductor are less frequent and have much larger amplitude [16].

6.1.3 Mechanism of formation of a noise field of DC line

Corona discharges on conductors, insulators or line hardware or sparking at bad contacts can be the source of radio interference as they inject current pulses into the line conductors. The corona current propagates along the conductors in both directions from the injection point. The various components of the frequency spectrum of these pulses have different effects. The radio interference voltages and currents propagating along the line produce an associated propagating electromagnetic field near the line (Figure 3). The fields near the line are related to the radio frequency voltages and currents propagating along the line, depending on the surge impedance of the line. Furthermore, the directions of the electric and magnetic field components are largely determined by the geometrical arrangements of the line conductors. In addition, the soil conditions affect differently the mirror image in the ground of the electric and magnetic field components, respectively.

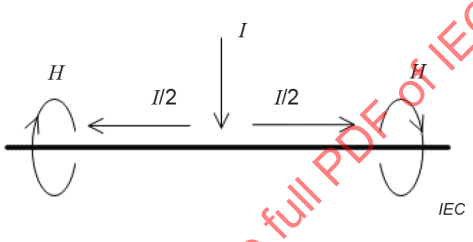

Figure 3 – The corona current *I* and radio interference magnetic field *H*

In the case of an HVDC line, the total electric field strength is the vectorial sum of the individual field strength components associated with each polar conductor. A more comprehensive treatment, together with practical methods of assessing the electromagnetic field, is needed.

6.1.4 Characteristics of radio interference from DC line

6.1.4.1 General

The radio interference characteristics of a high voltage DC line include frequency spectrum, lateral profile, statistical distribution.

6.1.4.2 Frequency spectrum

The spectrum is the variation of the radio interference measured at a given point in the vicinity of a DC line, as a function of the measurement frequency. Two phenomena are involved:

a) Current pulses

The current pulses generated in the conductors by the discharges show a particular spectrum dependent on the pulse shape. For this type of discharge the measured noise level falls as the frequency increases. In the range of broadcasting frequencies, where the positive discharges have a predominant effect, the spectrum is independent of the conductor diameter.

b) Attenuation

The attenuation of noise propagating along the line increases with frequency.

In the case of AC lines, the radio interference spectrum is one of the main characteristics of a high voltage line. The frequency spectrum for DC lines seems to show a similar shape to the AC lines over the long and medium wave broadcast bands but further investigations should be made.

6.1.4.3 Lateral profile

The RI field lateral profile of a bipolar HVDC line is nearly symmetrical about the positive conductor if the earth wires are corona-free. This behaviour can be explained by the fact that the negative conductor produces a lower level of radio interference than the positive conductor. With the same gradient for both conductors the difference in their radio interference level contributions is at least 6 dB. Hence radio interference from the negative conductors may be considered to be negligible. For a negative monopolar line, the noise level may be even 20 dB lower than for the same line with positive polarity.

6.1.4.4 Statistical distribution

The systematic study of fluctuations in the radio interference level of a line necessitates the continuous recording of the field strength under this line for at least a year at a fixed distance from the line and with a fixed measurement frequency. Numerous researchers, in many countries, have carried out such measurements with the result that there is in existence fairly reliable data on the annual or seasonal variations in radio interference level. These results are often presented according to statistical analysis methods, that is to say in the form of histograms or as cumulative distributions. The latter express the percentage of time during which the radio interference level was less than a given value.

The most important causes of fluctuations in recorded radio interference level are:

– the random nature of the phenomenon;
– variations of the meteorological conditions, both at the measuring point and along the few tens of kilometres of the line which contribute to the local interference;
– changes in the surface state of the conductors, which is affected not only by weather conditions such as rain and frost, but also by deposits of dust, insects and other particles.

6.1.5 Factors influencing the RI from DC line

6.1.5.1 General

The radio interference characteristics: level, frequency spectrum and lateral profile of a high voltage DC line are determined by:

– conductor surface conditions;
– conductor surface voltage gradient;
– polarity;
– weather conditions.

6.1.5.2 Conductor surface conditions

Research has shown considerably more fair-weather RI sources on DC lines compared to AC lines. During the late autumn and winter months, the fair-weather corona was low. In late spring and summer, the pattern of conductor corona sources repeated with corona increasing up to high levels.

6.1.5.3 Conductor surface gradient

One of the most important quantities in determining the radio interference level of a line, especially when conductor corona is dominant, is the strength of the electric field in the air at the surface of the conductor or surface voltage gradient.

All predictive formulae or analysis procedures for RI performance utilize the maximum conductor surface gradient (average maximum gradient of individual conductors in a bundle) as a prime parameter for estimating RI levels on DC and AC transmission lines. This variable is generally calculated from the physical geometry of the system and the system voltages in charge-free conditions. The conductor surface gradient calculated for charge-free conditions is a sensitive parameter for prediction of RI on AC lines. This is less so for DC lines. For example, on a conductor energized with AC lines, a change in operating voltage level of +10 % results in a change in RI of 5 dB or more for fair weather; in contrast, a change in DC operating voltage level of +10 % for practical line designs results in a change in RI of 3,5 dB.

6.1.5.4 Polarity

The positive pole of a bipolar HVDC line produces the greatest amount of RI to the extent that RI generation from the negative pole can be ignored. Therefore, RI generation is limited to specific conductors, unlike AC lines where all conductors are involved. Studies using conductor cages have shown RI generation from negative polarity conductors to be far below generation from positive polarity conductors. Positive polarity produces more RI than negative polarity because of fundamental differences in the corona processes. On positive polarity conductors, current pulses caused by corona have higher magnitude and longer decay times than on negative polarity. This results, at least in the broadcast band, in corona on positive polarity conductors affecting the broadcast band more than corona on negative polarity conductors. Additionally, in certain climates airborne surface contaminants were found in much greater proportion on the positive pole, causing higher RI generation.

6.1.5.5 Weather conditions

a) Fair/foul weather

Results from laboratories, tests, and operating DC lines have shown that the highest levels of RI occur during fair, dry weather rather than wet weather as for AC lines. During wet weather many water drops appear on the conductors. Water drops are very effective corona sources, because in an electric field they deform and become pointed, producing corona at electric fields much lower than the conductor surface electric field existing in corona-free conditions. Consequently, ionization of air near the surface of DC line conductors in wet weather is very intense and a significant amount of space charge is produced. This space charge increases corona loss and air ions, but also has the effect of producing a fairly uniform ion cloud around the conductors and of maintaining the actual conductor surface electric field at the relative low value of the water drop corona onset field. In these conditions, corona from water drops is not highly impulsive and noisy as the corona from sources in most fair weather conditions, but is more of a glow. Glow corona corresponds to a steady, noiseless charge emission from conductors into space. These phenomena do not occur for AC lines, because the polarity of the electric field near the conductor surface changes with power frequency, preventing the formation of a uniform ion cloud of the same polarity. Consequently, RI generation on DC lines is less during wet weather than in dry weather. It should be noted that there are exceptions to the rule that the highest RI levels occur during fair weather. Light snow, for instance, can produce slightly higher RI levels than dry weather.

Thus, the highest radio interference level of a DC line normally occurs under conditions of fair weather. At the beginning of rainfall and for dry snow precipitation, this level may rise for a short time but when the conductors are fully wet it will decrease by up to 10 dB and in some cases even more. The level may also be influenced by the line configuration and the voltage gradient and these remarks apply to bipolar and to positive monopolar lines. However, the 80 %/80 % criteria (the radio noise level does not exceed the limit for more than 80 % of the time with at least 80 % confidence) are still valid.

b) Rain washing

For AC and DC lines, the major effect of rain is to wash contaminants off the conductor surface. Because of space charge effects on DC lines, washing by rain can affect AC and DC fair weather RI differently. If the pre-rain RI level on DC conductors was a result of the activity of many RI sources close together with attendant space charge production which can lower RI by the formation of an effectively larger diameter conductor, then RI after washing on DC conductors could be higher than before. In contrast, rain washing always reduces the fair-weather RI level on AC lines.

c) Wind

Another area where the performance of DC lines differs from AC lines is the influence of wind. The influence of wind on the HVDC line may be notable. For a wind direction from the negative to the positive conductor the radio interference level increases with wind speeds over 3 m/s by 0,3 dB to 0,5 dB for each 1 m/s increment. For a wind direction from the positive to the negative conductor this effect is significantly lower.

d) Seasonal effects

Furthermore, the long-term radio interference level of a DC line is influenced by seasonal effects; in summer the level is normally higher than in winter by approximately 4 dB. This may be caused by insects and airborne particles on the conductor surface, or by the absolute humidity of the air.

6.1.5.6 Effect of altitude above sea level

With an increase in altitude, the air density is decreased, resulting in a decrease of corona-onset fields. This manifests also itself in RI levels: An increase in altitude results in an increase of RI levels of transmission lines as a consequence.

In [135] it was found that the RI at 0,5 MHz from HVAC lines is increased by about 1 dB every 300 m of increment in altitude above sea level. However, according to the latest research results in China [178] [179], the RI predicted by altitude correction formula proposed by China is much smaller than that predicted by the HVAC formula. Taking the RI at 0,5 MHz correction of ±500 kV transmission lines at 4 300 m elevation for example, the predicted value calculated by RI altitude correction method of HVAC is about 14,3 dB(μV/m), and the predicted value evaluated by RI altitude correction method of HVDC is about 10 dB(μV/m). The latter is only 70 % of the former.

6.2 Calculation methods

6.2.1 EPRI empirical formula

The radio interference characteristics: level, frequency, spectrum and lateral profile of an HVDC line are determined by: a) design parameters, b) line voltage, or conductor surface voltage gradient and polarity, c) weather conditions.

Monopolar RI prediction formulas were derived by EPRI and IREQ respectively [121] [122]. The EPRI empirical formula to calculate the monopolar RI for voltages up to 400 kV is given in Formula (20):

$$RI = 214\lg\left(\frac{g_{max}}{g_0}\right) - 278\left(\lg\frac{g_{max}}{g_0}\right)^2 + 40\lg(r) - 27\lg\frac{f}{f_0} - 40\lg\frac{D}{D_0} + 10\lg\left(\frac{\Delta f}{9}\right) \quad (20)$$

where

RI is the RI value to be calculated, quasi-peak value, dB above 1 μA/m$^{1/2}$;

g_{max} is the maximum surface voltage gradient, kV/cm;

g_0 is the onset surface voltage gradient, 14 kV/cm;

r is the radius of the conductor, cm;

f is frequency to be calculated, MHz;

f_0 is reference frequency (0,834 MHz);

D distance to the polar conductors (m);

D_0 reference distance to the polar conductors (30,5 m);

Δf reference bandwidth (5 kHz)

$$g_{max} = g_{av}\left[1+(n-1)\frac{d}{R}\right]$$

where

g_{av} is the average gradient of the bundle conductor, kV/cm;

R is the pitch-circle diameter of the subconductors;

n is the number of conductors in the bundle;

d is the diameter of subconductor, cm;

$$g_{av} = \frac{U}{\frac{nd}{2}\cdot \ln\frac{2h}{r_{eq}}}$$

where

U is the voltages on the conductors (kV);

h is the height of the conductor above ground, cm. Usually this is taken to be the mean of the heights at the two towers of the span minus 2/3 of the sag at the lowest point of the conductor;

r_{eq} is the radius of conductor or radius of bundle equivalent conductor (cm);

NOTE

a) $r_{eq} = d/2$ in the case of a single conductor;

b) $r_{eq} = \frac{R}{2}\sqrt{\frac{nd}{R}}$ in the case of a conductor bundle, R is the pitch-circle diameter of the subconductors.

6.2.2 IREQ empirical method

The IREQ empirical RI excitation function was developed for different seasons of the year as well as fair and foul weather conditions. This is given in Formula (21)

$$\Gamma = k_1 + k_2\cdot(g-g_0) + k_3\cdot \lg\left(\frac{d}{d_0}\right) + k_4\cdot \lg\left(\frac{n}{n_0}\right) \quad (21)$$

where

Γ is the RI excitation function in decibels over 1μA/m$^{1/2}$, quasi-peak value;

g is the maximum surface voltage gradient in kilovolts per centimetre;

n is the number of subconductors in the bundle;

d is the subconductor diameter in centimetres;

k_1, k_2, k_3 and k_4 are empirical constants;

g_0, n_0 and d_0 are reference values;

g_0 = 25 kV/cm, n_0 = 6, d_0 = 4,06 cm.

The parameters defining the excitation function developed by IREQ in [122] are given in Table 5 and Table 6. The empirical constant could not be defined in this study since only a single conductor was used as a reference.

Table 5 – Parameters of the IREQ excitation function (Monopolar) [122]

Polarity	Weather	k_1	k_2	k_3	k_4
+DC	Fair	33,29	2,28	-	–11,47
	Foul	31,7	1,69	-	–7,33
–DC	Fair	6,28	0,23	-	3,05
	Foul	6,3	0,46	-	–6,05

Table 6 – Parameters of the IREQ excitation function (Bipolar) [122]

Polarity	Weather	k_1	k_2	k_3	k_4
+DC	Fair	30,68	1,93	33,04	–11,44
	Foul	28,96	1,61	27,96	–7,37
–DC	Fair	22,42	1,86	24,13	–11,72
	Foul	22,05	1,53	20,40	–6,96

6.2.3 CISPR bipolar line RI prediction formula

CISPR recommended a bipolar line RI prediction Formula given in (22), which was based on extensive measurements on lines [14], with various configurations.

$$RI = 38 + 1{,}6\left(g_{\max} - 24\right) + 46\lg\left(r\right) + 5\lg\left(N\right) + \Delta E_f + 33\lg\left(\frac{20}{D}\right) + \Delta E_w \qquad (22)$$

where

RI is the level of the radio interference field strength, quasi-peak value, dB(μV/m);

$g_{\max}$ is the maximum surface gradient of the line, kV/cm;

r is the radius of conductor or subconductors, cm;

N is the number of subconductors;

D is the direct distance between antenna and nearest conductor, m;

ΔE_w is the correction for different weather condition, dB;

ΔE_f is the correction for different measurement frequency, dB, $\Delta E_f = 5\left[1 - 2\left(\log\left(10f\right)\right)^2\right]$;

f is the numerical value of the measurement frequency, MHz.

If the formula gives the level for 0,5 MHz and the position at a direct distance of 20 m from the nearest conductor in fair weather, then the last three elements of the formula are all zero.

6.3 Experimental data

6.3.1 Measurement apparatus and methods

This document applies to radio interference from DC overhead power lines and high-voltage equipment which may cause interference to radio reception, excluding the fields from power line carrier signals. The measurements need to be performed at such a distance from the HVDC converter stations that any corona from the station or converter generated interference will not impact the result. The frequency range covered is 0,15 MHz to 300 MHz. The measuring apparatus and methods used for checking compliance with limits conform to CISPR specifications, for example CISPR 16: CISPR Specification for Radio Interference Measuring Apparatus and Measurement Methods [123]. For the frequency range above 30 MHz, the measuring methods are still under consideration by CISPR although some basic aspects are given in CISPR 16.

The reference measurement frequency is 0,5 MHz. The following frequencies: 0,15 MHz; 0,25 MHz; 0,5 MHz; 1,0 MHz; 1,5 MHz; 3,0 MHz; 6,0 MHz; 10 MHz; 15 MHz; and 30 MHz can be used.

The test aerial is an electrically screened vertical loop, whose dimensions are such that the aerial will be completely enclosed by a square having a side of 60 cm in length. The base of the loop is generally about 2 m above ground. The aerial is rotated around a vertical axis and the maximum indication noted. If the plane of the loop is not effectively parallel to the direction of the power line, the orientation needs to be stated. The lateral profile of the radio interference field is to be determined. For purposes of comparison, the reference distance defining the noise level of the line is usually 20 m. Measurements is made at mid-span and preferably at several such positions. Measurements is not made near points where lines change direction or intersect. The atmospheric conditions need to be approximately uniform along the line. Measurements under rain conditions will be valid only if the rain extends over at least 10 km of the line on either side of the measuring site.

When the results of measurements are reported, the following additional information needs to be included at least: conductor surface voltage gradient; atmospheric conditions at measurement sites: temperature, pressure (altitude), humidity, wind speed, etc.; conductor configuration.

6.3.2 Experimental results for radio interference

The more and detailed experimental results for radio interference are shown in Annex B.

6.4 Criteria of different countries

No consistent criteria have been found around the world. No exact value for the RI limit of a AC line has been agreed by different countries. However one important line design principle for different organizations is to limit RI from DC lines in order not to influence broadcast reception. As a method to evaluate the RI of a DC power transmission line, the ratio of the received signal voltage to the received interference voltage (signal to noise ratio: SNR) is used, in the same way as for an AC transmission line.

$$\mathrm{SNR} = 20 \cdot \lg\left(V_{\mathrm{signal}} / V_{\mathrm{noise}} \right) \ [\mathrm{dB}]$$

The radio frequency SNR tests were conducted in line section 2 (4 × 30,5 mm with 11,2 m pole spacing). The broadcast station selected for the reception evaluation tests was CKWX, Vancouver, B.C., operating at 1 120 kHz, and quality of reception was evaluated at each of several test voltage levels in the range of ±300 kV to ±600 kV. At each test level, the evaluating panel (11 persons) assigned one of the following reception evaluations:

– background not detectable
– background detectable
– background evident
– background objectionable
– difficult to understand (hear)
– unintelligible.

The test result of reception quality versus SNR is shown in Figure 4. The subjective evaluations indicated DC RI tolerance level SNR of 10:1. Restated in terms of dB, the interfering noise at the receiving antenna is 20 dB below the broadcast signal strength for acceptable reception.

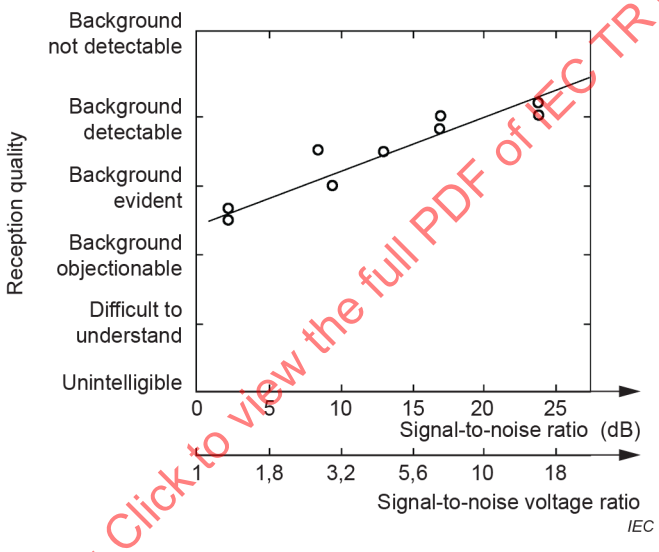

Figure 4 – RI tolerance tests: reception quality as a function of signal-to-noise ratio

In China, the consideration used for RI when doing HVDC line design is: when measurements are performed under fine weather conditions, they not exceed 55 dB(μV/m) at 0,5 MHz at the reference point, which is 20 m horizontally away from the centreline of the positive polarity conductor, and 2 m above ground.

7 Audible noise

7.1 Basic principles of audible noise

The intensity of a sound may be characterized by the root-mean-square amplitude of the small variations in atmospheric pressure that accompany the passage of a sound wave. It is usually expressed in terms of micro-pascals, abbreviated, μPa (1 μPa = 1 $\mu N/m^2$ = 10^{-5} μbar).

The range of pressure variations that the human ear can detect is extremely large (1 million to one).

For reporting convenience, a compressed scale has been devised on the basis of the logarithm of the sound pressure; this is the sound pressure level and is expressed in decibels above a reference pressure.

$$L_{ps} = 20 \lg \left(\frac{P_s}{P_r} \right) \quad [\text{dB}] \tag{23}$$

where

L_{ps} is the sound pressure level;

P_s is the sound pressure;

P_r is the reference pressure.

Unless otherwise specifically stated, the reference pressure is 20 µPa (2×10^{-4} µbar).

The human ear is not equally sensitive to all frequencies. Rather, it is more sensitive to the midrange frequencies where most speech information is carried. This characteristic is accounted for in sound measurements by adjusting the spectrum of the measured sound pressure level for the sensitivity of human hearing. In standardized sound measuring instruments, this is implemented with selectable A-, B-, C- and D- weighting networks [121], which give some frequencies more or less weight than some others. The characteristics of the different weighting networks are shown in Figure 5, along with the characteristics of the average human ear.

By far the most commonly used noise rating scale is the A-weighted sound level, expressed in dB(A). Although laboratory experiments by Wells [171], and by Molino [172] have indicated that subjective reaction to corona noise of HVAC lines might better correlate with the B- or D-weighting network, HVAC transmission line noise continues to be measured and reported in dB(A).

A study of the subjective response to HVDC transmission line audible noise [33] has concluded that, for the same dB(A) level, HVDC audible noise can create a different annoyance than HVAC audible noise; at 50 dB(A) HVDC and HVAC audible noises generate the same amount of annoyance, but at higher levels, HVDC audible noise is perceived as more annoying. Most practical HVDC lines produce audible noise of less than 50 dB(A) outside the right of way.

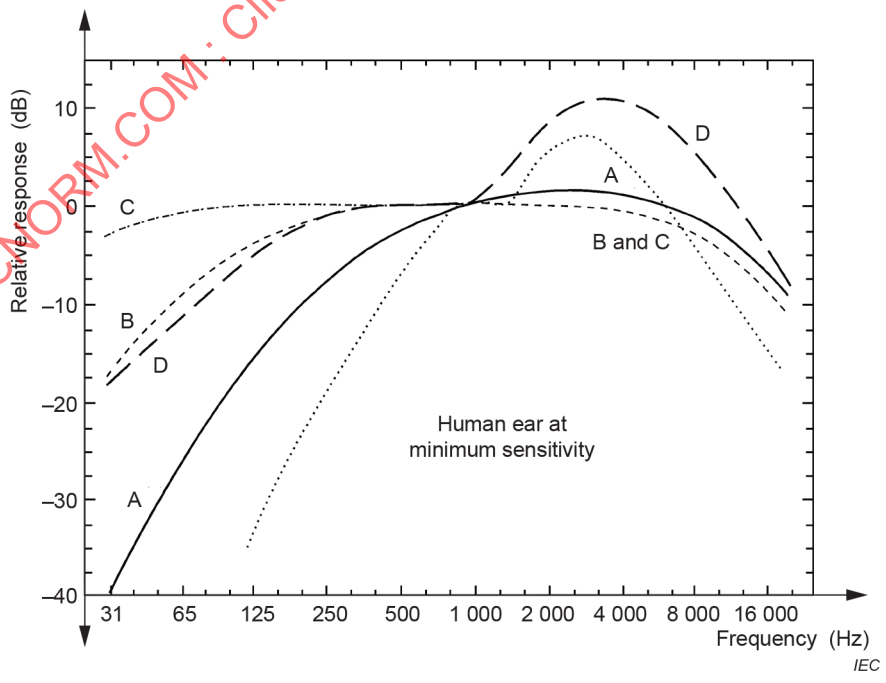

Figure 5 – Attenuation of different weighting networks used in audible-noise measurements [16]

7.2 Description of physical phenomena

7.2.1 General

Audible noise (AN) is one of the possible consequences of corona discharges occurring at the surface of conductors of overhead HVDC transmission lines. On rare occasions, audible noise is also produced by intermittent flashovers of insulator units in transmission line insulator strings.

Normally, HVDC transmission lines contribute very little to surrounding noise. Vehicles, aircraft, and industrial noise are more common sources. At operating voltages lower than ±400 kV, the noise level of practical HVDC transmission lines is of no concern. Even at operating voltages of ±400 kV or higher, audible noise from HVDC lines often can barely be distinguished from the general noise background, and it is difficult to measure separately from the background noise without special techniques.

Audible noise of HVDC lines occurs primarily in fair weather or during the transition from fair to foul weather. Therefore, HVDC line audible noise is of particular concern in areas where the ambient fair-weather noise is particularly low.

In most respects, HVDC transmission line audible noise is similar to that of HVAC transmission lines. Therefore, terminology and measuring techniques are the same as those used for HVAC transmission line audible noise [173].

Audible noise generated by corona on HVDC overhead transmission lines is broadband with significant high frequency content, which distinguishes it from more normal common surrounding noises. Corona is a random occurrence along the line and the noise from each corona pulse may extend to frequencies well beyond the sonic range. This randomness combined with the significant high frequency content results in sounds variously described as crackling, frying, or hissing. Figure 6 shows two typical frequency spectra of HVDC line corona noise measured at High Voltage Transmission Research Center (HVTRC) [132] one for a line configuration and voltage generating a relatively low audible noise and the other for relatively high corona noise conditions. A typical spectrum of fair weather ambient audible noise taken during the day is also shown for comparison. It is clear from Figure 6 that HVDC line audible noise measurements can be significantly affected by ambient noise. The low-frequency components of the noise (up to the 125 Hz octave band) can rarely be distinguished from ambient noise. The best indicators of corona noise are the octave band measurements from 500 Hz to 16 kHz. Unlike HVAC, HVDC corona noise does not contain pure tones at twice the power frequency and its harmonics.

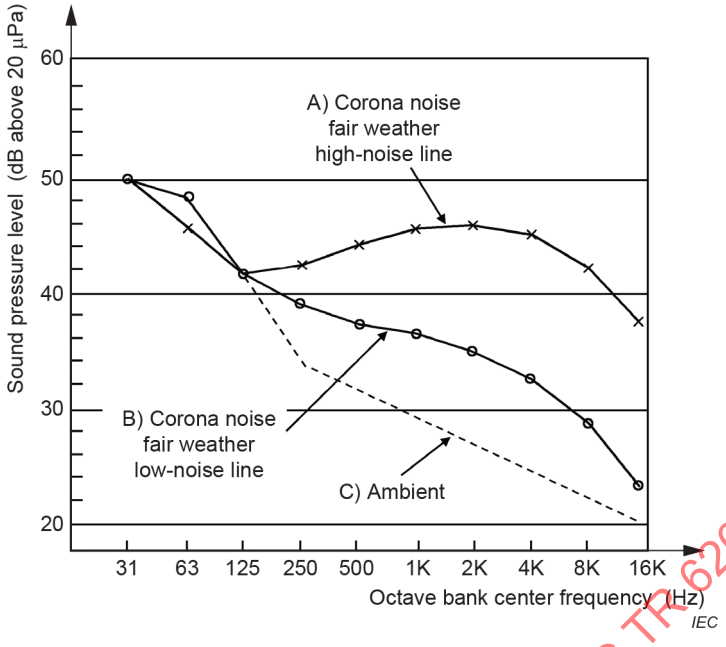

Figure 6 – Comparison of typical audible noise frequency spectra [132]

As sound waves travel through the air, there are mainly two kinds of noise attenuation terms, one is caused by geometric divergence, the other is caused by air absorption. The geometrical divergence accounts for cylindrical spreading in the free field from a line sound source, making the geometric divergence attenuation. A certain amount of energy is lost by molecular absorption resulting in attenuation. The absorption is a complex function of frequency, temperature, and relative humidity [174]. Air absorption is primarily important at the higher frequencies. At frequencies of 1 kHz to 2 kHz, it has a negligible effect. Typically, the absorption may result in a reduction of 1 dB to 2 dB of the A-weighted level for each 100 m of distance from the line noise source.

7.2.2 Lateral profiles

Typical lateral profiles of AN measured on an HVDC line energized to ±750 kV and ±900 kV equipped with 4 × 4,1 cm stranded round wires with a subconductor spacing of 45,72 cm are presented in Figure 7 [134]. The pole spacing is 13,72 m and the test line has average height of 16,58 m (minimum height of 13,72 m and a height of 22,31 m at the support points). The dashed curves in this figure correspond to the measured profiles obtained at the test line using a sound level meter equipped with a 1,27 cm microphone for outdoor operation, while the solid curves represent the profiles calculated using the generated acoustic power densities measured at these voltages and assuming that the noise comes mainly from the positive conductor.

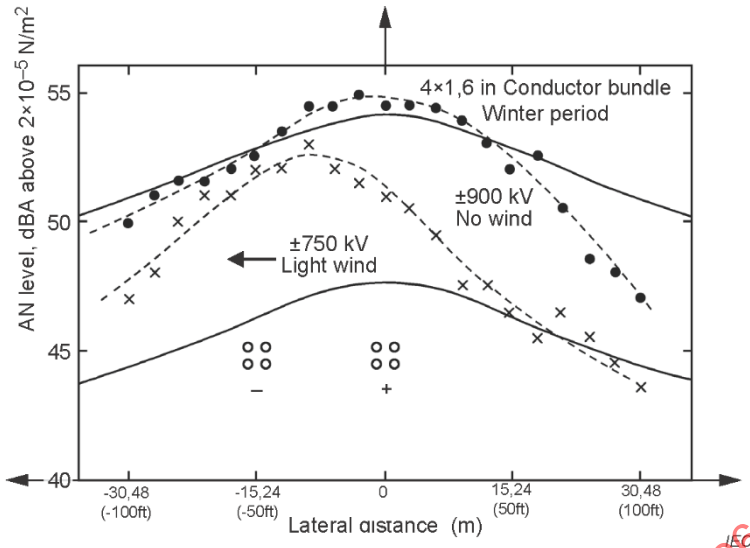

Bipolar HVDC-line equipped with 4 × 4,1 cm conductor bundles energized with ±750 kV and ±900 kV [134]

Figure 7 – Lateral profiles of the AN

Similar results are shown in Figure 8, where the experimental points as well as the calculated profile for the line are equipped with 8 × 4,6 cm conductor bundles energized to ±1 050 kV. The different points in Figure 8 correspond to different individual measurements.

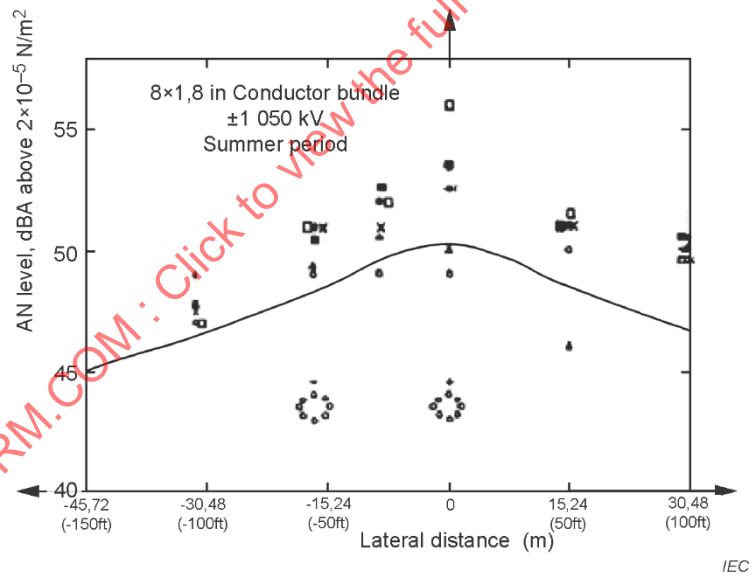

Figure 8 – Lateral profiles of the AN from a bipolar HVDC-line equipped with 8 × 4,6 cm (8 × 1,8 in) conductor bundles energized with ±1 050 kV [134]

The lateral profiles of AN measured under the test line agree reasonably well with those obtained using semi-empirical formulas.

As one can see from the profiles depicted in Figure 7 and Figure 8, the positive polarity conductor is the primary source of HVDC transmission line audible noise, as it is essentially symmetrical around the positive pole.

Figure 9 [132] shows the A-weighted lateral profiles measured under a test line energized at ±1 200 kV, ±1 050 kV and ±900 kV. There, only at the voltages of ±1 200 kV, the measured profile exhibits the expected behaviour with increased levels under the positive pole. Most probably, the ambient noise interferes with the lower audible noises from the line emitted at the lower voltages.

This would also explain the apparently weaker attenuation of noise levels measured far from the line energized with ±1 200 kV.

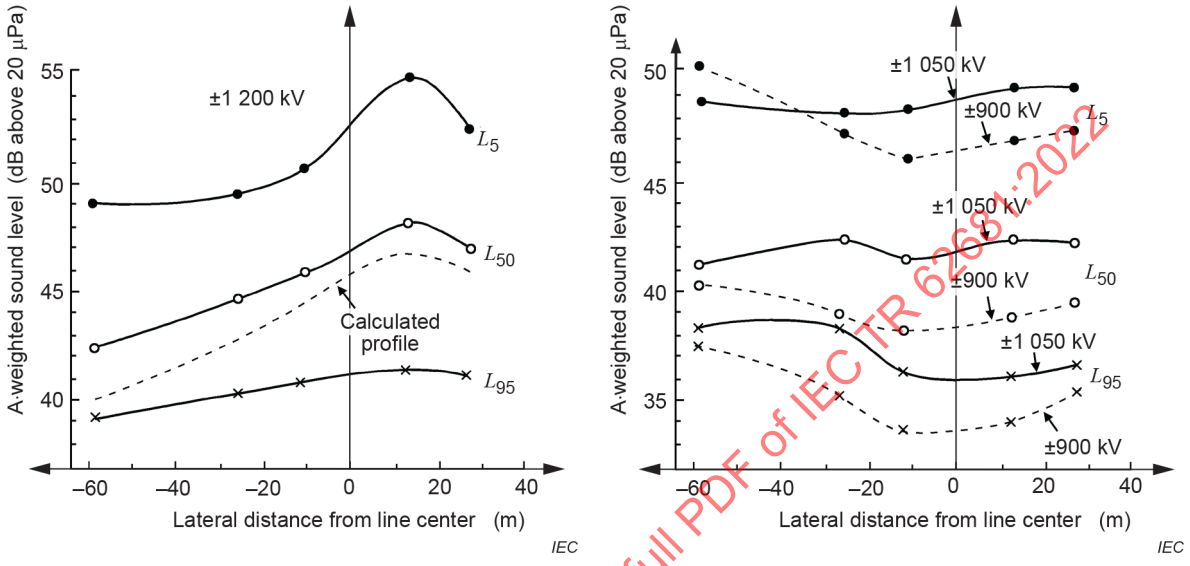

During Spring 1980 from a test line with 24,5 m pole spacing and 20 m distance to ground for different voltages [132]

Figure 9 – Lateral profiles of fair-weather A-weighted sound level [132]

From the profile of AN (Figure 7 and Figure 8), it can be seen that the profiles are symmetrical around the positive pole. It implies that positive polarity conductor is the primary source of AN from HVDC transmission line. This can be found in other literatures [8] [16] [34] [39] [122] as well. As the positive pole of a bipolar HVDC line produces relevantly more audible noise than the negative pole, the contribution from the negative pole can be ignored. For example, at a gradient of 25 kV/cm, test results using conductor cages have shown a difference between positive and negative polarity of about 8 dB [33]. Therefore, audible noise generation is limited to the positive pole, unlike in the AC case where all conductors are involved.

Positive polarity produces more audible noise than negative polarity because of fundamental differences in the corona processes. Similarly to the difference in the corona current pulse amplitudes between positive and negative polarity, the acoustic pulse amplitudes at positive polarity are also an order of magnitude higher than those at negative polarity. This asymmetry is enhanced by the fact that in certain climates airborne surface contamination and insects may both act as spots where corona sets in. They are found in much greater numbers on the positive pole.

7.2.3 Statistical distribution

The AN from HVDC transmission lines varies with the meteorological variables and the corona sources on the conductor surface. This variability can be quantified using the so-called exceedance levels such as L_{50} and L_5, which are widely used to assess AN from transmission lines. The summer fair-weather L_{50} is very useful in HVDC line design, because in summer the fair-weather AN is higher than in other seasons and weather conditions. Statistical descriptors are often applied to A-weighted sound levels. They are called exceedance levels or L-levels. For example, the L_5 is the A-weighted sound level exceeded for 5 % of the time over a specified time period. The other 95 % of the time, the sound level is less than the L_5. Similarly, the L_{50} is the sound level exceeded 50 % of the time; the L_{95} is the sound level exceeded 95 % of the time; etc.

In the following, two examples of assessing the audible noise from HVDC-lines with exceedance levels are presented to illustrate this statistical behaviour of the corona–noise.

Figure 10 [34] shows the all-weather probability distributions of AN at 15 m from the positive pole of the upgraded Pacific NW/SW HVDC Intertie by depicting the exceedance levels. For example, the fair weather L_{50} exceedance level in Figure 8 amounts to 41,0 dB (A).

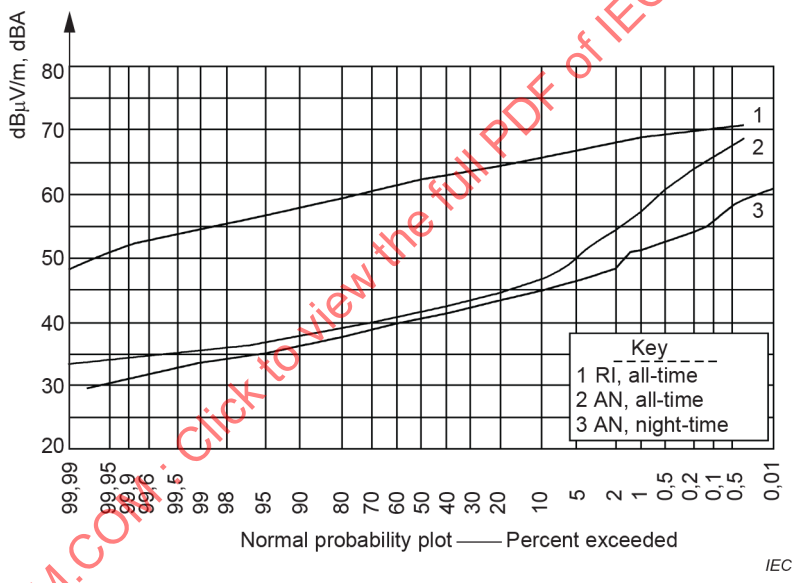

Figure 10 – All weather distribution of AN and RI at +15 m lateral distance of the positive pole from the upgraded Pacific NW/SW HVDC Intertie [34]

Figure 11 [132] shows the variability of the AN probability distributions for three different voltage levels. Only the measured values for the voltage ±1 200 kV are relatively undisturbed by ambient noise.

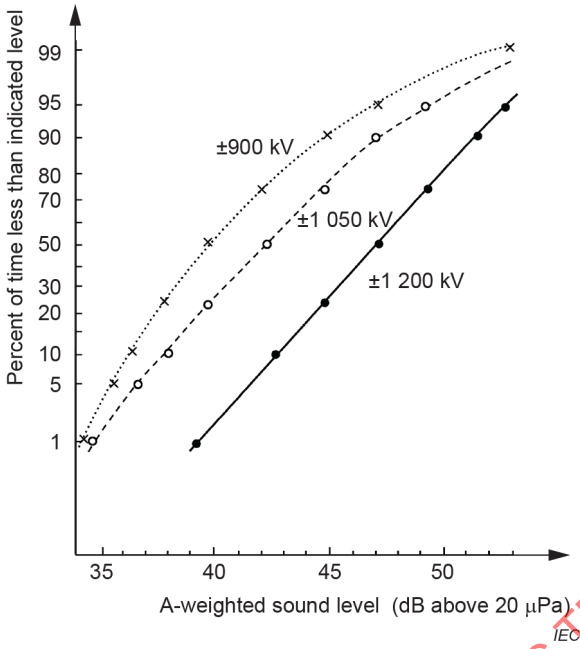

The pole spacing is 24,5 m, the minimum height of the horizontal pole arrangement above ground amounts to 20 m [132]

Figure 11 – Statistical distributions of fair-weather A-weighted sound level measured at 27 m lateral distance from the line centre during spring 1980

7.2.4 Influencing factors

7.2.4.1 Conductor surface gradient

All predictive formulae or analysis procedures for AN performance utilize the maximum conductor surface gradient as a prime parameter for estimating audible noise levels for DC (and AC) transmission lines. This variable is generally calculated from the physical geometry of the system and system voltages in charge-free conditions and is dependent on the line height, number and position of subconductors in the bundle, and separation of the subconductors. The conductor surface gradient calculated for corona-free conditions is a sensitive parameter for the prediction of audible noise. A change in dc operating voltage level of 10 % for practical line designs results in a change in fair weather audible noise of about 5 dB [121].

Much of the research on transmission line audible noise in the past has been devoted to HVAC transmission lines. The design considerations for HVAC [173] are similar to those for HVDC, but there are important differences for HVDC, such as the effect of constant polarity.

7.2.4.2 Conductor surface conditions

Research has shown considerably more fair-weather corona sources on HVDC lines compared with HVAC lines. Before rain, a density of less than three sources per meter has been reported for HVAC lines [173], On HVDC lines in dry weather up to 60 dead insects per meter were found at HVTRC. Visual observations show that positive conductors of HVDC lines are, in general, dirtier and collect more insects and debris than negative conductors. Nicks and scratches on a conductor can also act as a source of corona and audible noise.

7.2.4.3 Line polarity

The positive polarity conductor of a bipolar HVDC line produces more audible noise than the negative polarity conductor; in fact, audible noise generation from the negative pole is negligible and can be ignored. HVDC audible noise generation is limited to specific polarity conductors (positive polarity), unlike in the AC case where all conductors are involved due to the fact that AC conductors switch polarity 100 times per second and thus for half of their cycle have positive voltage.

Positive polarity produces more audible noise than negative polarity because of fundamental differences in the corona processes. On positive polarity conductors, current pulses caused by corona have higher magnitude and longer decay times than on negative polarity conductors. This results in more audible noise on positive polarity conductors than on negative polarity conductors. In addition, airborne surface contaminants and insects which can act as corona sources are found in much greater proportions on the positive polarity conductor.

7.2.4.4 Adjacent lines

The energization of nearby adjacent lines may affect the audible noise level produced by a conductor by modifying its surface gradient. All transmission lines in the same right-of-way need to be included in the calculation of conductor surface gradient. Adjacent AC lines can be considered as zero potential (grounded conductors) for purposes of DC noise calculation [163].

7.2.4.5 Weather parameters

Results from laboratories, test lines, and operating DC lines have shown that the highest levels of audible noise occur during fair, dry weather rather than wet weather as for ac lines. During wet weather, the degree of ionization on DC lines is sufficiently high so that surface irregularities of any sort are surrounded by space charge (corona-produced ions). The space charge acts to reduce the electric field at the surface of the conductor and the length of corona plumes, thus reducing the intensity of the corona current pulses; consequently, audible noise generation on DC lines is less during wet weather than in dry weather.

Essentially continuous HVDC corona emission occurs when the corona inception of the source is significantly lower than the corona-free conductor surface gradient. This is the case for raindrops, where the corona inception gradient for raindrops is approximately 9 kV/cm, while typical HVDC transmission lines operate at corona-free conductor surface gradients of approximately 20 kV/cm. In the case of near continuous corona emission, the corona current is either continuous or occurs in rapid small pulses that do not produce audible noise.

As a result of these phenomena, HVDC audible noise is a very complex function of the nature and number of corona sources. Both a source-free conductor and a conductor with many sharp sources (low corona inception field) produce little or no audible noise. The worst conditions occur when there is a critical number of noise-producing sources per unit of length. In fair weather, the number of sources per unit of length is usually below this critical number. In fair weather, a "dirtier" conductor is also a noisier conductor because it has more sources. In rain, however, the number of sources is well above the critical number producing sufficient corona and space charge such that the conductor surface self-shields itself reducing the length and duration of the individual corona plumes because of the surrounding space charge. This self-shielding by space charge results in a reduced audible noise level. During the transition from fair weather to rain, the noise of the conductor may first increase, then decrease, and practically disappear as the number of corona sources (raindrops) increases.

Fair weather audible noise will tend to increase as the amount of debris on the conductor increases. A gradual increase in the amount of debris and insects on the positive conductor is seen during the spring and summer of the year in temperate areas (such as HVTRC) where there are distinct summer and winter seasons. During autumn and winter, once the temperature falls consistently below about 10 °C, the number of insects and debris in the air and deposited on the positive conductor decreases. During autumn and winter, the debris on the conductor degrades and the conductor is cleaned by the action of snow, rain, and wind.

Wind can also have a slight effect on the audible noise of a conductor by carrying away the space charge released by corona. This decreases the amount of self-shielding of the conductor by its own space charge thus allowing longer corona plumes and more noise. The noise associated with the wind itself can produce a level that is equal to or more than noise from the DC line, masking the line noise.

7.2.5 Effect of altitude above sea level

With an increase in altitude, the air density is decreased, resulting in a decrease of corona-onset fields. This manifests also itself in AN levels: an increase in altitude results in an increase of AN levels of transmission lines as a consequence.

In [135] it was found that the audible noise from HVAC lines is increased by about 1 dB every 300 m of increment in altitude above sea level. However, according to the latest research results in China [180], the AN predicted by altitude correction formula proposed by China is much smaller than that predicted by the HVAC formula. From 0 m to 4 000 m, the AN increment of ±500 kV and ±600 kV HVDC transmission lines based on HVDC formula are 4,67 dB (A) and 7,07 dB (A) separately, which are much less than the predicted values by the AC method (13,33 dB(A)).

7.2.6 Concluding remarks

This Subclause 7.2 was primarily concerned with describing the characteristics of audible noise from HVDC transmission lines. The main results are summarized as follows.

a) The audible corona-noise from HVDC transmission lines originates mainly from the onset streamers from the positive pole. The acoustic pulses from the pulsative corona from both the positive and negative poles have similar shapes, but the amplitudes of the positive corona pulses are an order of magnitude larger than those of the negative polarity.

b) The frequency distribution of audible noise generated by corona on HVDC transmission lines is broadband with significant high-frequency content, whereas the common surrounding noises on the other hand have rather low sound levels.

c) The lateral profiles of AN from HVDC transmission lines is essentially symmetrical around the positive pole, which agrees with the remark a).

d) The occurrence of AN levels from HVDC transmission lines is to some extent distributed statistically, but is also connected with meteorological variables and the state of the conductor surface, i.e. the presence of protrusions. The variability can be characterized by means of exceedance levels. The L_{50} alone or in combination with L_5 exceedance levels are typically used to describe AN from transmission lines.

7.3 Calculation methods

7.3.1 General

The basic knowledge of generation, propagation and attenuation characteristics of audible noise is introduced in this Subclause 7.3. The commonly used semi-empirical formulas for predicting AN from HVDC transmission lines are summarized. They can be used in designing HVDC transmission lines.

7.3.2 Theoretical analysis of audible noise propagation

7.3.2.1 General

The audible noise from HVDC transmission lines occurs mainly during fair weather and is an important aspect in designing HVDC lines. There are two distinct calculation techniques for AN from transmission lines: the comparative and the analytical methods.

7.3.2.2 Comparative methods

These methods usually are derived from measured data on lines having the same general configuration but having different conductor geometries or different voltage levels.

The line geometry of a new line is compared with that of a reference line of similar characteristics for which measured data are already available, and correction factors are applied to the measured data to translate from the reference line to the new line. The general form of the calculations for the comparative method is [16] [121] [159]:

$$L_{\mathrm{p}} = L_{\mathrm{AN0}} + \Delta AN_{\mathrm{g}} + \Delta AN_{\mathrm{d}} + \Delta AN_{\mathrm{n}} + \Delta AN_{\mathrm{R}} + \Delta AN_{\mathrm{A}} + \Delta AN_{\mathrm{W}} \tag{24}$$

where

L_{AN0} is the audible noise level of the reference line

ΔAN_{g} is the correction factor related to corona free conductor surface gradient

ΔAN_{d} is the correction factor related to diameter of conductors

ΔAN_{n} is the correction factor related to number of conductors per bundle

ΔAN_{R} is the correction factor related to distance from line to measuring point

ΔAN_{A} is correction factor related to altitude above sea level

ΔAN_{W} is correction factor related to weather conditions

7.3.2.3 Analytical methods

The propagation of AN can be analyzed using the basic law of acoustics. The noise level produced by each conductor bundle can be calculated at the point of measurement. Once the noise for each conductor bundle is obtained, the total line noise (in dB) is found from [16].

$$P = 10\lg\sum_{i=1}^{n} 10^{P(dB)_i/10} \quad [\mathrm{db}] \tag{25}$$

where

P(dB) is the predicted noise level in dB,

n is the number of conductor bundles,

$P(\mathrm{dB})_i$ is the noise level in dB of bundle i.

7.3.3 Empirical formulas of audible noise

The empirical formulas are related to the comparative methods. The formulas are usually developed by regression equations expressed as a function of the conductor maximum surface gradient, the number of sub-conductors, the diameter of the sub-conductors and the radial distance between the conductor and the measuring point. They can be used reliably only for lines having same general configuration as those from which the measured data were obtained. For example, if all data were obtained from a single circuit bipolar HVDC transmission lines, they would be invalid for double circuit bipolar HVDC transmission lines.

7.3.4 Semi-empirical formulas of audible noise

7.3.4.1 General

The semi-empirical formulas are related to the analytical methods. To calculate the corona-generated sound pressure, two factors must be considered: the generated acoustic power density of the line and the propagation characteristic of the audible noise.

Only, the positive polarity is assumed to produce noise. The noise of the negative polarity is assumed to be negligible. If there is more than one positive conductor bundle, the audible noise at any particular point is calculated by combining the noise produced by each bundle and then combining them according to Equation (25).

If there is only one positive polarity conductor, such as for an ordinary bipolar HVDC line, there is no need to use Equation (25), since the negative polarity conductor contribution to the audible noise is negligible.

The following formulae are all applicable to the case of straight and infinite transmission lines.

7.3.4.2 EPRI formula

The EPRI formula for L_{50} AN from DC lines according to the data obtained at HVTRC of EPRI [16] in summer fair weather is given as:

$$A_{50} = -57{,}4 + 124 \lg\left(\frac{g}{25}\right) + 25 \lg\left(\frac{d}{4{,}45}\right) + 18 \lg\left(\frac{n}{2}\right) + k_n \tag{26}$$

A_{50} is the generated acoustic power in dB above 1 W/m.

Considering the effect of air absorption and geometrical spreading, the following expression for summer fair weather can be drawn:

$$L_{50} = 56{,}9 + 124 \lg\left(\frac{g}{25}\right) + 25 \lg\left(\frac{d}{4{,}45}\right) + 18 \lg\left(\frac{n}{2}\right) - 10 \lg R - 0{,}02R + k_n \tag{27}$$

where

g is the average maximum bundle gradient [kV/cm]

d is the diameter of conductors [cm]

n is the number of conductors per bundle

R is the radial distance from the positive conductor to the measuring point with an assumption that the power line is infinite and straight [m], the height of the conductor is usually taken as the average height as the actual line is usually in the shape of catenary.

k_n is the adder function of the number n of conductors in a bundle:

k_n = 0, for $n \geq 3$; k_n = 2,6, for n = 2; k_n = 7,6, for n = 1.

The range of validity is considered to be 15 < g < 30 kV/cm, 2 < d < 5 cm and 1 < n < 6.

The AN in wet weather is calculated by subtracting 6 dB from the L_{50} summer fair weather noise, while the summer fair weather exceedance level L_5 can be calculated by adding 6 dB to the corresponding L_{50} (the noise exceeded for 50 % of the time [dB(A)]) fair weather noise level [16].

The L_{50} AN for winter fair weather can be calculated by subtracting 4 dB from the L_{50} summer fair weather, while the corresponding L_{50} level for spring and fall fair weather can be calculated by subtracting 2 dB from the L_{50} summer fair weather level.

7.3.4.3 BPA formula

BPA uses the existing HVDC line audible noise data from IREQ (three different line geometries at 750 kV, 900 kV, and 1 050 kV), from BPA (two different line geometries at 533 kV and 600 kV) and from the Square Butte line (250 kV), which formed the basis to develop a more general formula for AN from HVDC lines [146].

Considering the effect of air absorption and geometrical spreading, the following expression can be developed for fair weather in the fall months:

$$L_{50} = -133{,}4 + 84 \lg(g) + 40 \lg\left(d_{\text{eq}}\right) - 11{,}4 \lg R \tag{28}$$

where

g is the average maximum bundle gradient [kV/cm].

d_{eq} is the equivalent bundle [cm]

$$d_{\text{eq}} = \begin{cases} d \cdot 0{,}66 n^{0{,}64} & \text{for } n > 2 \\ d & \text{for } n \leq 2 \end{cases}$$

d is the diameter of conductors [cm]

R is the radial distance from the positive conductor to the measuring point with an assumption that the power line is infinite and straight [m], the height of the conductor is usually taken as the average height as the actual line is usually in the shape of catenary.

The range of validity is considered to be $3 < d < 5$ cm and $1 \leq n \leq 8$.

To correct the calculation for summer, 2 dB (A) is added to the L_{50} fall value. The maximum fair weather AN is calculated by adding 3,5 dB to the L_{50} fair weather value obtained above, while the L_{50} AN during rain is calculated by subtracting 6 dB from the L_{50} fair weather AN.

7.3.4.4 FGH (Germany) formula

This formula calculates the maximum audible noise in fair weather:

$$L_{\text{max}} = -1 + 1{,}4g + 40 \lg d + 10 \lg n - 10 \lg R \tag{29}$$

where

L_{max} is the maximum audible noise in fair weather, in dB above 20 µPa.

R is the distance between the positive pole and the measuring point.

The range of validity is considered to be $2 \leq d \leq 4$ cm, $2 \leq n \leq 5$.

7.3.4.5 IREQ (Canada) formula

The IREQ (Canada) Formula is given by the Hydro Quebec Institute of Research [8] [141] [146]:

$$L_{50} = k\left(g - 25\right) + 10 \lg n + 40 \lg d - 11{,}4 \log_{10} R + AN_0 \tag{30}$$

where

L_{50} is the average audible noise in fair weather, in dB above 20 µPa.

R is the distance between the positive pole and the measuring point.

The k and AN_0 depend on the season are illustrated in Table 7.

Table 7 – Parameters defining regression equation for generated acoustic power density [8]

Season of the year	Weather conditions	AN_0	k
Summer	Fair	26,5	1,54
Autumn/Spring	Fair	26,6	0,84
Winter	Fair	24,0	0,51

The range of validity is considered to be $2 \le d \le 4$ cm, $2 \le n \le 5$.

7.3.4.6 The CRIEPI (Japan) formula

From Central Research Institute of Electric Power Industry, Japan, the following formula exists [145]:

$$L_{50} = AN_0 - 10\lg R \tag{31}$$

where

L_{50} is the average audible noise in fair weather, in dB above 20 µPa

R is the distance between the positive pole and the measuring point

g is the average maximum bundle gradient [kV/cm]

$$AN_0 = 10\frac{G_{60}}{G_{60} - G_{50}}\left[1 - \frac{G_{50}}{g}\right] + 50$$

in which G_{50} and G_{60} represent bundle gradients which correspond to AN_0 = 50 dB(A) and AN_0 = 60 dB(A) respectively, and are given by

$$\frac{1}{G_{50}} = \frac{\lg n}{91} + \frac{\lg d}{19} + \frac{1}{2w^2} + \frac{1}{151}$$

$$\frac{1}{G_{60}} = \frac{\lg n}{72} + \frac{\lg d}{21} + \frac{1}{2w^2} - \frac{1}{1906}$$

where

w is the distance between positive and negative poles in meters.

The range of validity is considered to be $2{,}24 \le d \le 4{,}94$ cm, $1 \le n \le 4$, $w \ge 8{,}44$.

Besides, the calculation method of AN in consideration of Fmax (the true maximum conductor surface gradient in the presence of space charge) has been developed [143].

7.3.5 Concluding remarks

In 7.3.4.2 to 7.3.4.3 introduced formulae, the BPA formula and EPRI formula are the most widely used in the design of HVDC transmission lines, and it is reasonable to determine which formula is in better agreement with a planned transmission line by tests with a laboratory setup that reflects the lines technical parameters. The EPRI formula is commonly used for the design because it is developed based on the long-term research of audible noise from HVDC and UHVDC transmission lines.

7.4 Experimental data

7.4.1 Measurement techniques and instrumentation

The instrumentation required to make audible noise measurements is composed of three basic components: a transducer (microphone) to convert acoustical pressure into electrical signals, a processing device to weight and/or filter the electrical information, and an output device to determine the levels of the acoustical signals. The equipment available to perform these measurements varies significantly in sophistication from simple, hand-held instruments to complex, computer-controlled systems. Transmission line noise measurements are unique in that, generally, they require the measurement of low noise levels, they are concerned with noise with high frequency content, and they must be performed outdoors. These requirements affect the measurement system with regard to sensitivity and frequency response.

When more detail is desired than can be provided by a simple measure of the noise (e.g. A-weighted), a complete determination of the frequency spectrum is made using frequency analyzers. For field measurements, an octave-band filter set is often used. For better definition, narrow-band frequency analyzers with one-third or one-tenth octave filters are also used. One octave is defined as a bandwidth for which the ratio between upper and lower frequency of the band is 2.

For the one-third and one-tenth octave bands, the ratios are $\sqrt[3]{2}$ and $\sqrt[10]{2}$, respectively. As the bandwidth is increased, the pressure level measured for random noise (having a flat spectrum within the band) is proportional to the square root of the bandwidth.

The microphone is an important part of the noise-measuring system. There are several types and sizes of microphones available. Each has its own characteristics, and thus its own advantages and disadvantages. If the characteristics of a given microphone and the basic characteristics of the noise being measured are understood, the limitations of a particular microphone can then be determined. As long as these limitations are recognized and adjustments for them are made, the particular type of microphone used is not of major importance. For measurement of audible noise during rain, some means of microphone protection will be required for all but the very shortest-duration measurements.

The measurements of audible noise are made with a microphone located 15 m laterally from the positive pole of the HVDC transmission line and 1,5 m above ground at the midspan of the line. The microphone is oriented so that the axis of the microphone diaphragm is pointed at the conductors of the transmission line.

7.4.2 Experimental results for audible noise

The more and detailed experimental results for audible noise are shown in Annex C.

7.5 Design practice of different countries

7.5.1 General

The tolerability of audible noise depends on the characteristics of the noise and on the level of ambient noise. The most important difference between HVAC and HVDC audible noise is that potentially objectionable HVAC audible noise occurs in foul weather while potentially HVDC audible noise occurs in fair weather. Because people are more frequently outdoors in fair weather and as there is no rainfall masking the corona noise, as in the case of HVAC, it is favourable to minimize the number of complaints.

Transmission line audible noise has been an issue in many public hearings on-line certification applications [12]. The New York State Public Service Commission Cases 26529 and 26559 “Common Record Hearing on Health and Safety of Extra-High Voltage Transmission Lines” requires the L50 rain limit level of 52 dB at the boundary of the right of way [12]. In the Chinese 1 000 kV UHVAC transmission line pilot project, an average foul weather AN limit value is 55 dB (A) at 20 m distance to the outer conductor. For HVDC, there is a limited amount of experience because, in general, audible noise has been sufficiently low and no reported complaints have been made known to bodies such as CIGRE. However, because HVDC audible noise occurs in fair weather, limits consistent with minimizing the number of complaints need to be adopted for it.

7.5.2 The effect of audible noise on people

The effects of audible noise on humans are mainly manifest on speech, hearing, sleeping and emotional response.

a) The sound level of speech is about 60 dB(A). Speech will be typically interfered with when noise exceeds a level of 65 dB(A), and noise levels exceeding 90 dB(A) can make speech unintelligible.

b) The primary effect of prolonged exposure to high levels of noise such as more than 80 dB(A) in the workplace results in the development of industrial or occupational deafness; this is often called noise-induced hearing loss.

c) Interference with periods of rest or sleep results in lack of concentration, irritability or reduced efficiency as a consequence. Normal sleep of about 15 % of people is affected when the audible noise levels are higher than 50 dB(A). A study by EPRI [14] found that the sound of the power transmission line was more effective in awakening people than other sounds used in the study. Exposure to the power line at levels of about 10 dB(A) to 15 dB(A) lower than surrounding sounds led to an equal probability of awakening.

d) Finally, the exposure to unaccustomed high levels of noise tends to change emotional responses. People tend to become more agitated or less reasonable. There is also some evidence that noise is associated with mental illness. In particular, it can lead to general psychological distress.

7.5.3 The audible noise level and induced complaints

The first reported assessment of the impact of HVAC transmission line audible noise was by Perry in 1972 [14]. This guideline is illustrated in Figure 12 which shows that no complaints are likely under 52,5 dB (A), some complaints can be expected between 52,5 and 59 dB (A) and numerous complaints have to be anticipated if the levels exceed 59 dB (A).

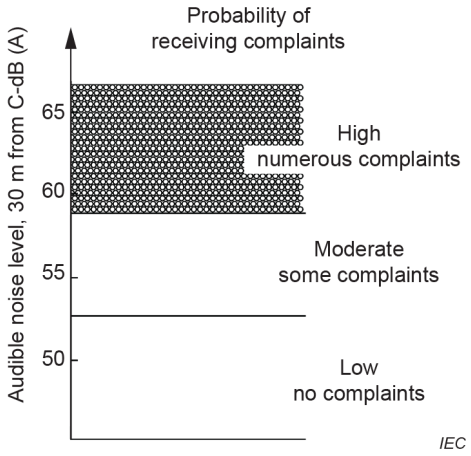

Figure 12 – Audible noise complaint guidelines [14] in USA

An investigation by EPRI [136] used an acoustic-menu technique to determine subjects' preference for different types of noise, including transmission line noise and more commonly encountered noises. One of the conclusions was that variability of individual relative annoyance judgments of low level (45 dB(A) to 55 dB(A)) signals is greater than variability in judgments of the annoyance of higher-level signals. One of the other conclusions of this study was that the annoyance produced by exposure to transmission line noise is greater than that of other low-level signals of similar A-level. AN of transmission lines and other low-level sounds with appreciably high frequency content result in the same annoyance as other surrounding sounds at 10 dB lower levels. The same increase of annoyance for equal noise levels occurs for noises with tonal components as that at twice the mains frequency from HVAC lines.

CEPRI has conducted some research on the human subjective response to transmission line audible noise in high altitude area [152]: Figure 13 is the measured lateral profile of audible noise on a 330 kV AC transmission line. At the point of AN greater than 45 dB (A), 85 % of evaluators feel disturbed.

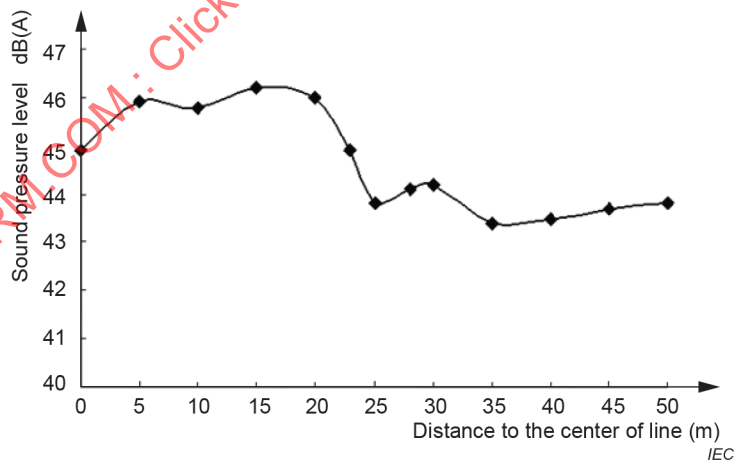

Figure 13 – Measured lateral profile of audible noise on a 330 kV AC transmission line [152]

Another investigation conducted by EPRI [14] to determine the human subjective response to HVDC transmission line audible noise was conducted directly under the positive polarity conductor, and voltage covered the range of ±300 kV to ±600 kV. At each test voltage level, the evaluators were requested to rank the annoyance in one of the following categories:

1) very quiet still, calm
2) quiet just a normal quiet evening

3) fairly noisy some moderate disturbance
4) noisy just plain noise
5) very noisy very prominent on this quiet evening
6) intolerably noisy.

The test results of this investigation are shown in Figure 14 and Figure 15. The evaluators in USA felt annoyed when the average noise level exceeds 45 dB (A).

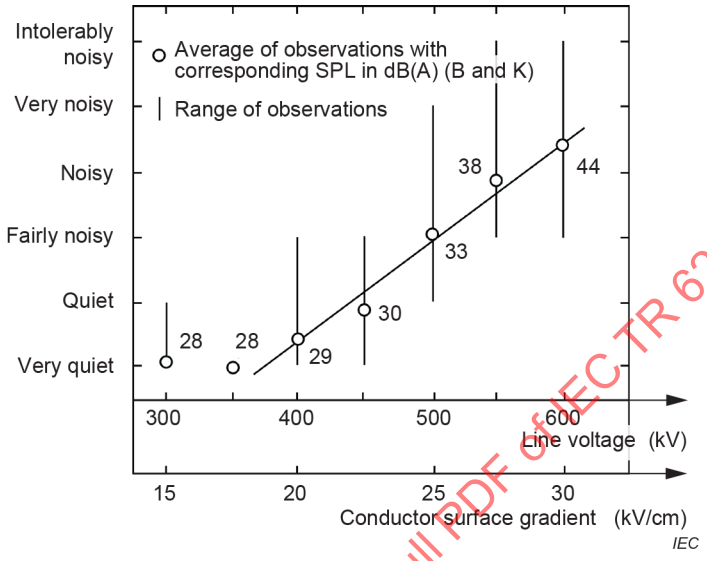

Figure 14 – Subjective evaluation of DC transmission line audible noise; EPRI test centre study 1974 [14]

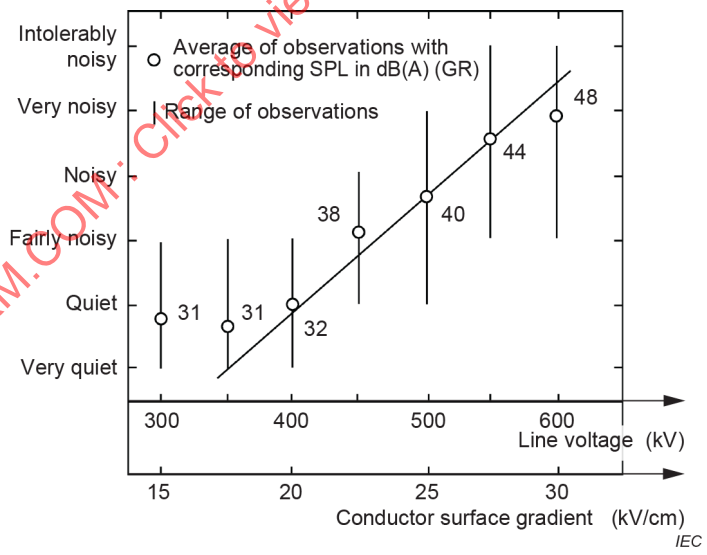

Figure 15 – Subjective evaluation of DC transmission line audible noise; OSU study 1975 [14]

A study of the effect of the different characteristics of HVAC and HVDC noise [14] has shown that the correlation between annoyance and dB (A) is very strong for AC line but less so for DC lines. Around 50 dB (A), DC and AC audible noise generates about the same amount of annoyance.

For levels of noise lower than 50 dB (A), corresponding to those generally produced by HVDC lines, DC audible noise generates less annoyance than the corresponding AC-noises of the same level. Therefore, extending the use of the A-weighted HVAC limit levels to HVDC lines seems to be conservative under the aspect of annoyance.

The research of subjective evaluation AN was also carried out by M. Fukushima et al. [145] on the SHIOBARAN HVDC test line. One of the main results is that if the AN level exceeds 43 dB (A), the rate of test persons perceiving it as "noisy" rises to more than 50 %. If the value exceeds 45 dB (A), this rate is increased to more than 70 % (see Figure 16). That ambient noise plays an important role in how the HVDC noises are perceived becomes manifest in Figure 17.

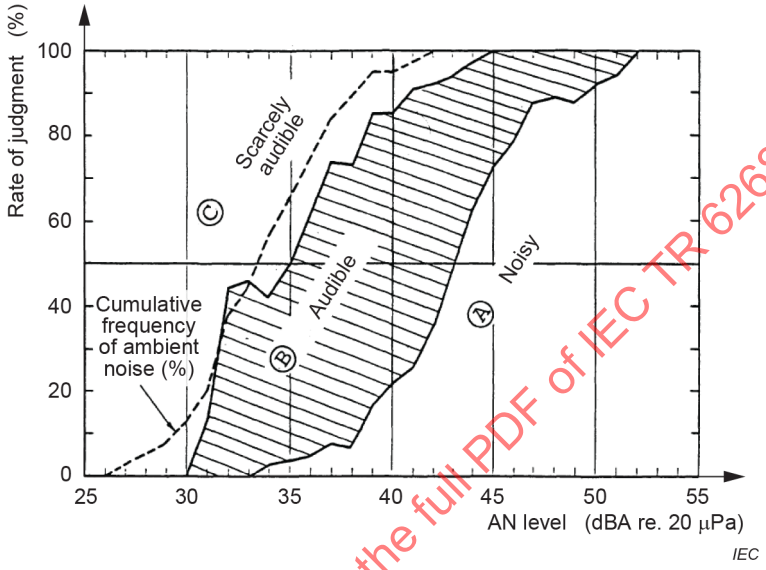

The judgments were made 74 times at operating voltage for conductor bundles of 1 × 4,94 cm and 1 × to 4 × 2,53 cm by two of the authors aged in their 20's and 30's [145].

Figure 16 – Results of the operators' subjective evaluation of AN from HVDC lines

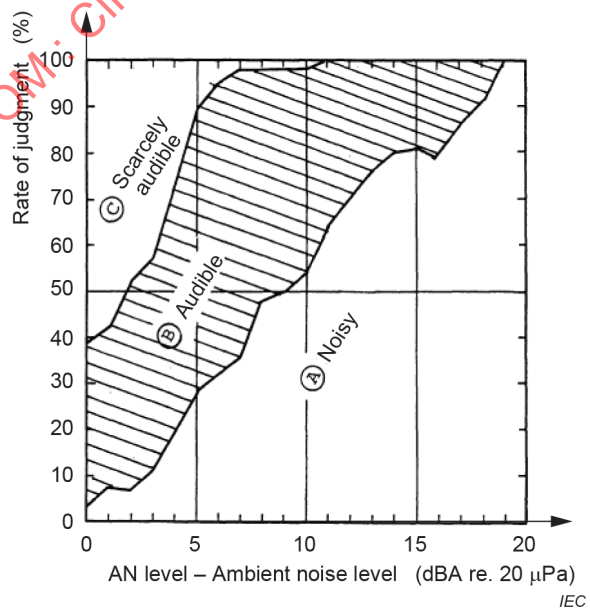

Rate of judgment versus relative difference between AN level and ambient noise level [145]

Figure 17 – Results of subjective evaluation of AN from DC lines

All this research indicated that 45 dB (A) with a quiet background from HVDC transmission line will be perceived as “noisy” and may result in some complaints.

7.5.4 Limit values of audible noise of HVDC transmission lines in different countries

The United States Department of Energy (USDOE) study [16] suggests a guideline of 40 dB(A) to 45 dB(A) for the 50 % fair weather noise of HVDC lines, against a 50 dB(A) to 55 dB(A) for the 50 % foul weather noise of HVAC lines. This suggestion is based on earlier investigations by the Bonneville Power Administration (BPA) [33] in dictating that 40 dB(A) is a level above which noise from HVDC lines may be considered as objectionable.

In Brazil the limit for AN of HVDC transmission lines on the boundary of the right of way is L_{50} = 40 dB(A).

In the Chinese electric power industry standard [154], the limiting exceedance level L_{50} at 20 m lateral distance from the positive pole at mid-span is 50 dB (A). However, the recommended AN limit by CEPRI is lower, namely L_{50} = 45 dB (A) at 20 m lateral distance from the positive pole at mid-span in fair weather for ±800 kV UHVDC transmission lines above 1 000 m and in non-residential 50 dB (A) are acceptable [152].

The Japanese limit for AN of HVDC transmission lines is L_{50} = 40 dB (A).

7.5.5 General national noise limits

Cost and feasibility need to be taken into account in considering the limit value of audible noise.

General noise requirements of the national surrounding noise regulations need to be satisfied and the audible noise needs to be limited to the public acceptance level. In designing the HVDC transmission lines, on the other hand, the construction cost will be a matter of consideration as well.

In the noise regulations in Germany and Switzerland transmission lines are not specially treated with specifically limiting noise levels, but they are implicitly covered by the more general regulations on noise. In German regulations on noise [155] (TA-Lärm), for very sensitive areas such as hospitals the outdoor limits are 45 dB(A) in the daytime (06:00 to 22:00) and 35 dB(A) to 70 dB(A) at night (22:00 to 06:00) depending on the sensitivity of the area. It is specific that these night limits are to be fulfilled for every L_{eq}(A) averaged over any full hour during the night (if the events are not unique or very seldom), in contrast to the more common requirements of averaging over a longer period.

The limits for very sensitive areas are the same in Switzerland (planning values) [156] and in China [157], namely 50 dB (A) and 40 dB (A) in the daytime and at night respectively.

It must be pointed out that due to the different methods in determining the levels in the different national regulations mentioned above, the levels cannot be compared directly.

Values of sound attenuation by a residential house with opened windows can vary widely.

However, reference [158] quantifies this attenuation in warm weather with 12 dB(A), see Table 8.

Table 8 – Typical sound attenuation (in decibels) provided by buildings [158]

	Window opened	Window closed
Warm climate	12	24
Cold climate	17	24

Annex A
(informative)

Experimental results for electric field and ion current

A.1 Bonneville Power Administration ±500 kV HVDC transmission line

The Bonneville Power Administration (BPA) study [34] to characterize the electrical surroundings of the Pacific NW/SW HVDC Intertie was carried out at the Grizzly Mountain HVDC Research Facility. The test site was located at an altitude of 1,1 km and the line configuration consisted of a two-conductor bundle, with 46,2 mm diameter subconductors, pole spacing of 11,6 m and conductor height of 12,2 m.

Ground-level electric field intensity, ion current density and space charge density were measured at several lateral distances from the line, using Institut de Recherche d'Hydro Quebec (IREQ) field mills and Wilson plates, and Dev Industries ion counters. Measurements were made at lateral distances of 7,9 m, 22,9 m, 152 m and 305 m on both sides from the centre of the line. Data were obtained with the line operating at ±500 kV during a period of one full year in 1986.

Statistical analysis of the data indicated that all-weather results were very similar to fair-weather results, since foul weather occurred less than 10 % of the time. All-weather results for lateral distances of 7,9 m and 22,9 m under both positive and negative poles are summarized in Table A.1.

Both the mean values, E (mean), J (mean), and the L_5 values (exceeded 5 % of the time), E (L_5), J (L_5), of the ground-level electric field intensity and ion current density are shown in the table.

An important conclusion drawn from this study was that the distribution of electric fields and ion current densities were very much asymmetric, with the levels on the negative side of the line being two to three times higher than those on the positive side. Such asymmetry was not observed in the case of some test line data obtained in other studies.

Table A.1 – BPA ±500 kV line: statistical summary of all-weather ground-level electric field intensity and ion current density [34]

Parameter measured	Lateral distance, m			
	−22,9	−7,9	7,9	22,9
E (mean), kV/m	−10,7	−17,7	10,5	6,5
E (L_5), kV/m	−23,0	−34,0	20,0	15,0
J (mean), nA/m^2	−10,2	−29,3	12,8	3,6
J (L_5), nA/m^2	−50,0	−112,0	46,0	18,0

A.2 FURNAS ±600 kV HVDC transmission line

The FURNAS ±600 kV HVDC transmission line configuration consists of a four-conductor bundle, with a subconductor diameter of 34,17 mm and bundle spacing of 45,7 cm, pole spacing of 16,6 m and minimum conductor height of 13,5 m.

Ground-level electric field intensity, ion current density and charge density were measured at several points laterally on both sides of the line [38]. Monroe vibrating plate sensors were used for electric field measurement. The sensors were used in an inverted position and placed above ground planes, mainly to prevent them from being short-circuited during periods of precipitation. Ion current density was measured using Wilson plates and space charge density was measured using a Dev ion counter. Although ion current density was measured at ground level, electric field and space charge density were measured above ground.

The measurement program was carried out during four separate one-month periods in 1996 and 1997. A statistical summary of the electric field intensity E and ion current density J at different lateral distances is presented in Table A.2. The results show some degree of asymmetry, with the values under the negative pole being higher than those under the positive pole, although not to the same extent as in the case of the BPA line.

Table A.2 – FURNAS ±600 kV line: statistical summary of ground-level electric field intensity and ion current density [38]

Parameter measured	Lateral distance, m										
	−36	−28,3	−18,3	−13,3	−8,3	0	8,3	13,3	18,3	28,3	36
E (L_{50}), kV/m	−10,2	−18,4	−27,6	-	−34,5	2	25,2	-	18,2	11,3	4,5
E (L_5), kV/m	−23,8	−45,6	−60,3	-	−72,6	4	44,7	-	32,8	23,1	13,5
J (L_{50}), nA/m^2	−9,1	-	−19,5	−27	−37,9	-	19,4	11,9	26,5	-	3,5
J (L_5), nA/m^2	−31,3	-	−111,4	−88	−108,1	-	53,8	87,4	68,6	-	14

A.3 Manitoba Hydro ±450 kV HVDC transmission line

A coordinated corona performance study was carried out [39] on Bipoles 1 and 2 of the Nelson River HVDC transmission system of Manitoba Hydro. These two bipoles run parallel to each other and are separated by about 65 m. Each bipole consists of two-conductor bundles, with a subconductor diameter of 40,6 mm and bundle spacing of 45,7 cm, pole spacing of 13,4 m and minimum conductor height of 12,2 m.

A Wilson plate and field mill developed at IREQ were used to measure the ground-level ion current density and electric field intensity respectively. The measurement program was carried out over a period of only four days on one of the bipoles operating at ±450 kV. Due to the unavailability of a number of instruments, the same Wilson plate and field mill were moved from point to point to obtain lateral profiles.

Typical lateral profiles of the electric field intensity and ion current density for bipolar operation of the line (with wind flowing from negative to positive pole with velocity of 1,0 m/s) are shown in Figure A.1. The measurements were taken by placing the instruments at each point and making about 25 to 50 data scans lasting from two to four minutes. The observed asymmetry in the distributions may be attributed partly to wind as shown in Figure A.1.

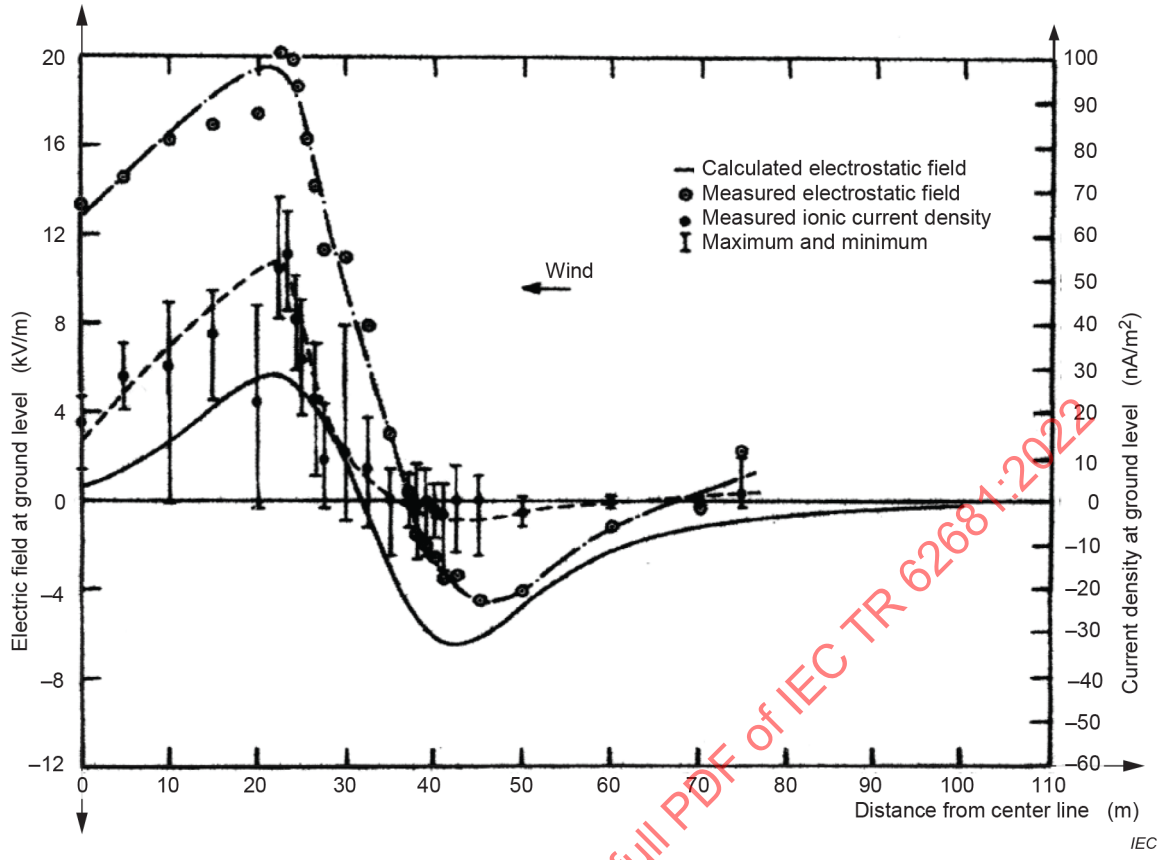

Figure A.1 – Electric field and ion current distributions for Manitoba Hydro ±450 kV Line [39]

Continuous measurements of electric field intensity and ion current density were made with the instruments placed one metre away from under the positive pole for monopolar and bipolar operation of the line during a period of two days. Similar measurements were also made with the instruments placed about one metre away from under the negative pole, but during a period of only one day. Cumulative probability distributions of the electric field intensity and ion current density obtained from a statistical analysis of the data are shown in Figure A.2 and Figure A.3.

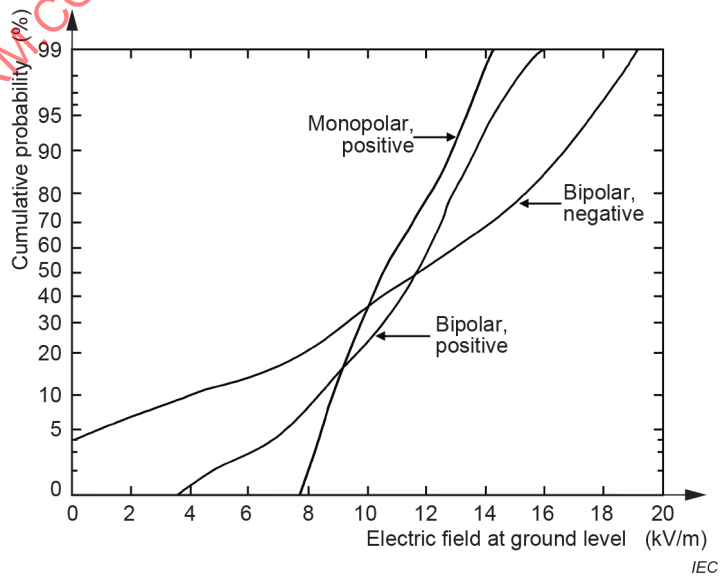

Figure A.2 – Cumulative distribution of electric field for Manitoba Hydro ±450 kV Line [39]

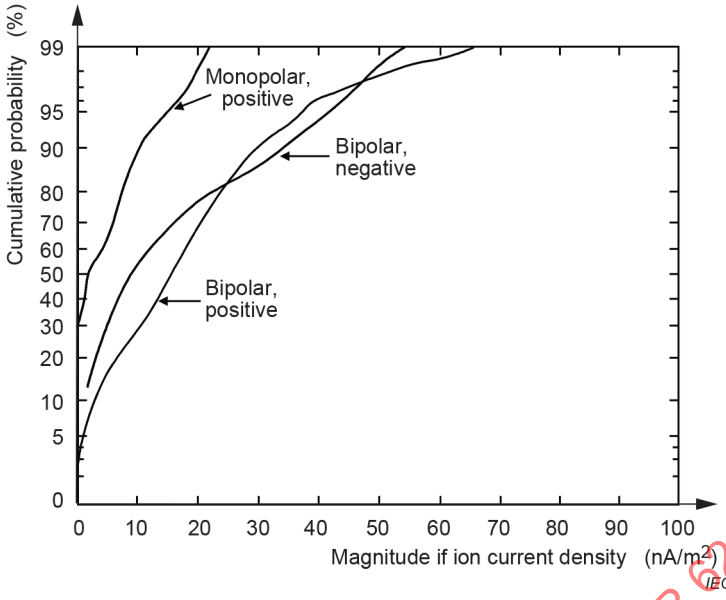

Figure A.3 – Cumulative distribution of ion current density for Manitoba Hydro ±450 kV line [39]

The usefulness of the experimental data obtained in this study is somewhat limited because of the short duration of the tests and the fact that measurements at different points to determine lateral profiles were not made simultaneously.

A.4 Hydro-Québec – New England ±450 kV HVDC transmission line

Data were collected as part of a long-term comprehensive program to monitor electric and magnetic fields and ions before and after energization of this ±450 kV HVDC transmission line. Each pole conductor consists of a 3-conductor triangular bundle, with pole spacing of 13,7 m, and a minimum conductor height of 14,6 m above ground at the monitoring locations. Monitoring of the electrical surroundings and commenced at Bath, NH in December 1988 and Hudson, NH in April 1989 on an existing right-of-way and continued after energization of the DC line on this right-of-way in July 1990 for another two years ending in November 1992 [40]. A summary of the pre-construction measurements have been published [41].

Measurements of electric field, ion concentrations of both polarities and aerosol concentrations were measured at two FAR stations located +46,6 m and −51,8 m from centreline at the site in Bath, NH with a self-contained meteorological station location adjacent to one of the stations. There are also other instruments measuring electric field and ion current density at the approximate locations of peak values just outside the conductors (NEAR stations at +10,7 m and −10,7 m). The same parameters were measured at FAR sites (+29,0 m, −50,3 m) and NEAR sites (+8,5 m, −8,5 m) around the line at the southern site in Hudson, NH but the pole spacing at that site was 9,5 m.

The results (Table A.3 and Table A.4) from the northern site in Bath, NH are summarized below based on the report January 1992 to October 1992 in [41].

Table A.3 – Hydro-Québec–New England ±450 kV HVDC transmission line. Bath, NH; 1990-1992 (fair weather), 1992 (rain), All-season measurements of static electric E-field in kV/m [41]

Weather	Parameter measured	Distance, m			
		−51,8	−10,7	+10,7	+46,6
Fair	E (L_{50})	−0,3	−5,5	8,4	1,2
	E (L_5)	−2,5	−13,1	17,2	3,5
Rain	E (L_{50})	−0,4	−6,2	7,4	1,1
	E (L_5)	−3,4	14,6	15,6	3,4
Bath, NH; 1990-1992 (fair weather), 1992 (rain), All-season measurements of static electric E-field in kV/m					

Table A.4 – Hydro-Québec – New England ±450 kV HVDC Transmission Line. Bath, NH; 1990-1992, All-season fair-weather measurements of ion concentrations in kions/cm^3 [41]

Weather	Parameter measured	Distance m		Distance, m	
		−51,8	−10,7	+10,7	+46,6
Fair	+ Ions (L_{50})			14	0,6
"	+ Ions (L_5)			81	5,1
"	− Ions (L_{50})	0,3	5,0		
"	− Ions (L_5)	1,8	46		
Bath, NH; 1990-1992, All-season fair-weather measurements of ion concentrations in kions/cm^3					

A.5 IREQ test line study of ±450 kV HVDC line configuration

Corona studies were carried out on the test line at IREQ [43] in order to determine the pole spacing and minimum conductor height for the ±450 kV bipolar DC transmission line interconnecting Hydro Quebec with the New England Power pool in 1986. A four-conductor bundle, with a 35,6 mm diameter subconductor and 45,7 cm bundle spacing, was used for this line. Following an initial study on the test line to investigate the influence of varying pole spacing and conductor height on the ground-level electric field and ion current distributions, IREQ recommended the selection of the following design parameters for the proposed line: pole spacing of 11 m and minimum conductor height of 13 m.

In a second phase of the study, the IREQ test line was configured with these recommended values of pole spacing and minimum conductor height and long-term corona performance tests were carried out for the duration of about one year. IREQ field mills and Wilson plates and Dev ion counters were used to measure the ground-level electric field intensity, ion current density and space charge density at several points laterally at the centre of the line. Statistical analysis was carried out on the long-term test data and the mean values μ_E, μ_J and standard deviations σ_E, σ_J respectively of the electric field intensity and ion current density at different measurement points and under all-season fair weather and foul weather conditions are summarized in Table A.5.

The results obtained in this study are not presented in the form of cumulative distributions and, strictly speaking, do not provide the L_{50} and L_5 levels of the ground-level electric field intensity and ion current density. However, if the data are assumed to follow Gaussian distribution, the L_{50} values will correspond to the mean values shown in Table A.3 and the L_5 values can be determined as equal to (μ + 1,645σ), where μ is the mean value and σ is the standard deviation of the parameter considered.

Table A.5 – IREQ ±450 kV test line: statistical summary of ground-level electric field intensity and ion current density [43]

Season and weather	Parameter measured	Lateral distance, m								
		−30	−20,5	−5,5	−2,75	0	2,75	5,5	20,5	30
All-season Fair weather	μ_E (kV/m)	−4,76	−8,63	-10,45	-	2,92	-	11,39	6,13	2,45
	σ_E (kV/m)	3,25	4,04	4,17	-	1,76	-	5,43	2,74	2,22
	μ_J (nA/m^2)	−1,6	-5,0	−10,2	-3,5	1,1	6,6	10,5	0,7	0,3
	σ_J (nA/m^2)	1,9	5,4	10,1	5,1	3,2	8,6	11,8	1,5	1,2
All-season Foul weather	μ_E (kV/m)	−4,81	−10,08	−13,82	-	4,5	-	13,85	8,8	4,93
	σ_E (kV/m)	3,55	5,34	6,84	-	2,45	-	8,26	4,8	3,64
	μ_J (nA/m^2)	−0,8	-3,4	−10,2	−5,9	0,5	10,6	13,4	1,7	1,1
	σ_J (nA/m^2)	1,5	5,9	12,9	9,9	3,2	15,9	17,0	2,1	1,6

A.6 HVTRC test line study of ±400 kV HVDC line configuration

The ground-level electric fields and ion currents of a bipolar DC line configuration, used on the CPA-UPAN HVDC transmission line in Minnesota and North Dakota, were studied on the test line at the High Voltage Transmission Research Center (HVTRC) in Lenox, MA [44]. The conductor configuration was a twin conductor bundle using 3,82 cm conductors with a 45,7 cm spacing. Three different values of pole spacing (9,15 m, 12,2 m and 15,2 m) were tested at two mid-span heights (10,7 m, 15,2 m). Long-term measurements were made over a period of about six months (20 May to 4 December, 1981), with the voltage maintained at ±400 kV except for occasional voltage-runs (varying the line voltage from zero to the maximum value, slightly above the normal operating voltage) of limited duration.

The test line was monitored with instrumentation for measuring electrical and climatic parameters. The electric field and ion current instrumentation consisted of arrays of electric field and ion current sensors located laterally under the line at mid-span. The ion current sensors were Wilson plate type collectors with 1 m^2 collecting surface and 7,5 cm guard ring. The plates were elevated 24 cm above ground, which results in an equivalent collecting surface area of about 1,4 m. The electric field sensors were vibrating-element type field probes. They were operated in an inverted mode about 30 cm above ground to prevent weather related failure due to rain or snow. Each electric field sensor assembly is calibrated through comparison in fair weather of its reading against the reading of a sensor operated in a conventional manner at ground level. Thirteen electric field and ion current monitoring stations were located at mid-span perpendicularly to the line. The stations were located at positions −48 m, −33 m, −23 m, −13 m, −8 m, −3 m, 2 m, 7 m, 12 m, 17 m, 37 m and 52 m.

Table A.6 gives the 5 %, 50 % and 95 % values of the electric field and ion current at the positive and negative peaks of the lateral profiles for all of the six-line configurations studied during various weather conditions. The effect of line height on the electric fields and ion currents is readily seen while the pole spacing has less effect. The weather dependence of the electric fields and ion currents is also evident.

Table A.6 – HVTRC ±400 kV test line: statistical summary of peak electric field and ion currents [44]

Pole spacing (m)	Line height (m)	E_{max+}			E_{max-}			J_{max+}			J_{max-}		
		5 %	50 %	95 %	5 %	50 %	95 %	5 %	50 %	95 %	5 %	50 %	95 %
Fair Weather													
9,15	15,2	9,1	14,0	18,3	−3,1	−6,7	−12,0	3,6	13,7	30,5	+0,2	−3,1	−20,0
9,15	10,7	11,3	21,3	26,3	−7,3	−11,9	−19,0	2,7	47,8	83,5	−1,4	−14,8	−49,7
12,2	15,2	7,3	13,5	18,3	−3,8	−8,8	−16,0	2,2	13,6	32,7	−0,1	−6,9	−26,4
12,2	10,7	14,5	23,5	29,6	−9,4	−15,8	−27,4	13	64,1	120	−2,8	−26,2	−108,6
15,2	15,2	7,0	13,3	19,5	−4,7	−9,0	−16,2	2,0	16,2	36,7	+0,2	−4,5	−25,2
15,2	10,7	16,5	22,7	28,2	−7,8	−13,5	−21,7	15,4	54,7	113,6	−1,5	−17,1	−63,2
Fog													
9,15	15,2	7,8	14,3	18,3	−6,8	−12,3	−18,3	5,4	13,9	31	−6,3	−14,8	−36,1
9,15	10,7	17,4	23,9	28,8	−13,0	−22	−29,4	37,9	66	116,6	−21,9	−64,1	−135,1
12,2	15,2	8,4	13,8	21,4	−9,9	−15,0	−19,8	3,8	15,8	34,4	−9,2	−25,0	−40,3
12,2	10,7	19,5	24,9	33,3	−20,8	−27,6	−32,6	46,7	83,6	149,4	−65,6	−115,5	−163,2
15,2	15,2	9,0	15,3	21,2	−7,9	−14,7	−29,7	6,0	17,3	45,6	−5,7	−25,4	−49,5
15,2	10,7	20,1	25,1	30,8	−15,8	−23,2	−31,3	35,1	72,3	154,9	−17,9	−73,1	−147,6
Rain													
9,15	15,2	12,0	18,0	20,9	−6,7	−13,5	−18,8	8,3	27,5	60,4	−4,0	−28,6	−51,1
9,15	10,7	20,5	24,8	28,4	−16,9	−26,2	−30,8	35,8	101,7	138,0	−33,1	−101,0	−150,9
12,2	15,2	13,0	16,6	18,9	−9,1	−17,0	−19,7	13,8	36,4	53,9	−6,3	−30,0	−51,4
12,2	10,7	22,0	29,6	33,7	−14,6	−27,7	−31,7	30,3	103,2	175,7	−23,0	−93,5	−168,5
15,2	15,2	15,8	19,1	20,7	−13,3	−20,4	−29,5	17,9	37,8	59,6	−18,8	−41,1	−61,2
15,2	10,7	17,4	28,7	32,5	−9,9	−31,2	−34,2	19,2	106	114	−2,9	−101,5	−167
Snow													
15,2	15,2	6,9	11,8	15,0	−10,9	−13,3	−17,2	1,1	8,6	15,5	−4,7	−10,7	−18,0
12,2	10,7	13,0	20,8	24,0	−17,9	−22,4	−28,3	19,3	52,4	77,0	−40,5	−70,9	−123,6
12,2	15,2	6,0	10,2	13,5	−5,9	−11,6	−15,5	0,9	7,6	13,9	−0,1	−8,2	−17,7
Frost													
15,2	15,2	10,5	19,5	33,5	−6,5	−14,0	−21,8	11,8	46,0	121,9	−8,6	−34,7	−110,8
15,2	10,7	20,5	28,1	34,4	−9,8	−13,6	−22,4	46	72,2	125,9	−14	−35	−168

NOTE Ion currents are actual plate readings; to obtain the ion current densities, the readings are divided by 1,4 m^2.

A.7 Test study in China

Before the implementation of a UHVDC project, a test study on the electromagnetic surroundings of ±800 kV UHVDC lines with a conductor bundle of 6 × 720 mm^2 has been carried out for one and a half years, by making use of the UHV DC test lines at Beijing.

Tests on the total electric field at ground level have been carried out under different weather conditions, when three kinds of conductors with different quantities are adopted. The conductor pattern is 6 × 720 mm^2. The pole spacing is 22 m, and the minimum conductor height is 18 m. Table A.7 shows the results obtained after the statistical analysis for hundreds of thousands of test data. Data shown in Table A.7 will be improved and adjusted with the continuation of test.

It could be concluded from Table A.7 that the statistical average level of the total electric field is almost |–30| kV/m or below under at the negative conductor side, except in December and the period during which wind is small. The result in spring is the smallest, and that in summer is a little larger. At the positive conductor side, the statistic average values of the total electric field in winter and in spring are lower than 30 kV/m. The total electric field is bigger at the positive conductor side, which is related to the larger humidity in summer.

Table A.7 – Statistical results for the test data of total electric field at ground (50 % value) [119]

Season		Negative (kV/m)	Positive (kV/m)
Summer	2007.7	−32	35
Winter	2007.12	−38	30
	2008.1	−27	18
Spring	2008.3	−27	20
	2008.5	−25	23

The test shows that the humidity obviously influences the total electric field. The increase of humidity leads to the increase of the total electric field at the positive conductor side, and the decrease at negative conductor side. The statistical result of the total electric field at different humidity reflects this phenomenon, which is shown in Figure A.4. The calculation result of the total electric field for conductors in dry air is consistent with that for conductors in air of moderate humidity (60 % to 70 %), as shown in Figure A.5. The Xiangjiaba-Shanghai and Jinping-Sunan ±800 kV DC lines are located in the south of China, and the humidity is high in summer. According to the test, it is necessary to apply correction factors to the minimum conductor height given by the calculation. The extent of the increase is about 7 %.

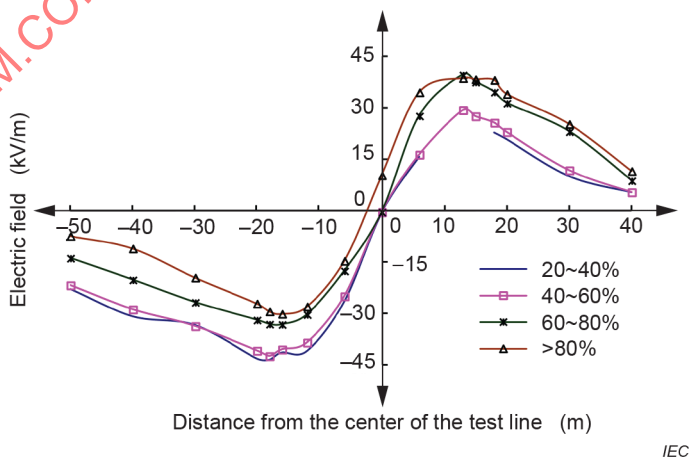

Figure A.4 – Test result for total electric field at different humidity [119]

The effect of some other factors on the total electric field at ground are also statistically analyzed, including wind speed, temperature, the conductor pollution level and conductor machining quality, etc. The calculation method of the total electric field of UHVDC lines will be continuously improved in future.

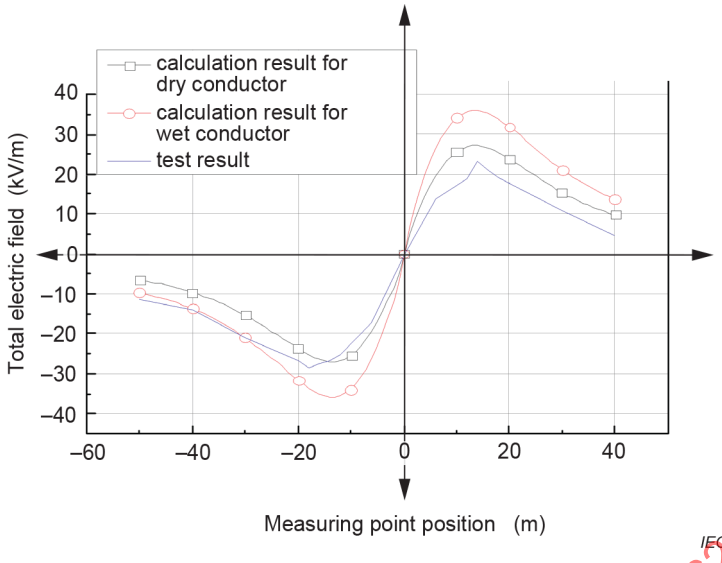

Figure A.5 – Comparison between the calculation result and test result for the total electric field (minimum conductor height is 18 m) [119]

Annex B
(informative)

Experimental results for radio interference

B.1 Bonneville power administration's 1 100 kV direct current test project

B.1.1 General

The earliest experiments of DC RI came from the Bonneville Power Administration's 1 100 kV Direct Current Test Project, which was from about 1963 to 1964 [124]. This test lines arrangement was like Figure B.1. All RI measurements were obtained with Stoddart NM 20B radio interference meters using the quasi-peak (QP) detector with the Stoddart bandwidth was 6 kHz.

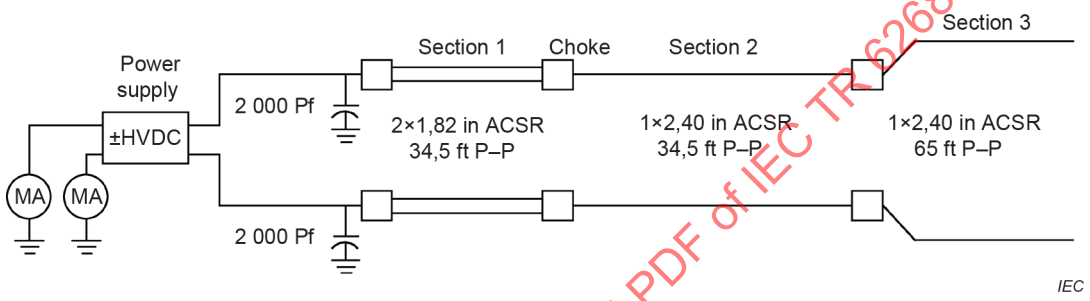

Figure B.1 – Connection for 3-section DC test line [124]

B.1.2 Lateral profile

A typical RI lateral profile at 0,834 MHz for bipolar 600 kV operation of Line Section 2 (5-bundles, 30,5 mm at 11,2 m pole spacing) is shown in Figure B.2.

The RI produced by the negative pole is typically about one-half (−6 dB) the RI produced by the positive pole and the negative pole's contribution to the total bipolar RI level is negligible. Therefore, note that the profile is essentially symmetrical about the centreline of the positive-polarity conductor.

Figure B.3 illustrated the highest RI levels occurred under the positive conductor. The lateral attenuation in the three line sections was essentially the same, i.e. RI is inversely proportional to 1/(radial distance to conductor) out to approximately 45,72 m (150 ft).

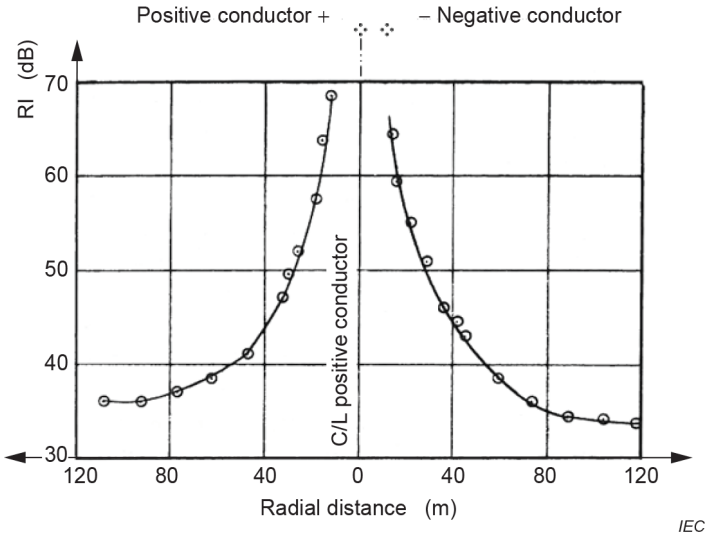

Figure B.2 – Typical RI lateral profile at ±600 kV, 4 × 30,5 mm conductor, 11,2 m pole spacing, 15,2 m average height [14]

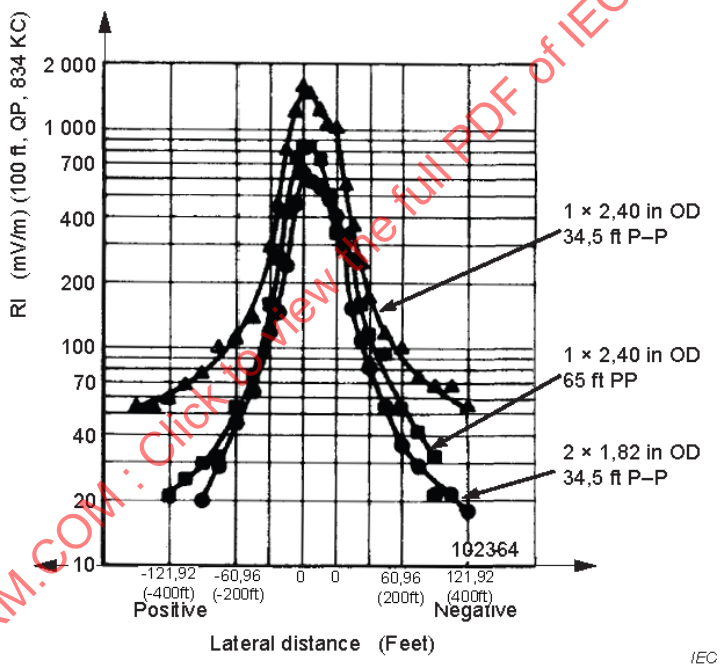

Figure B.3 – Simultaneous RI lateral, midspan, in clear weather and light wind for three configurations, bipolar ±400 kV [124]

B.1.3 Influence of conductor gradient

The relationship between RI and conductor gradient for Line Section 2, with 11,2 m pole spacing is illustrated in Figure B.4. These data were taken at the midpoint of the tested span, 30,5 m from the positive conductor.

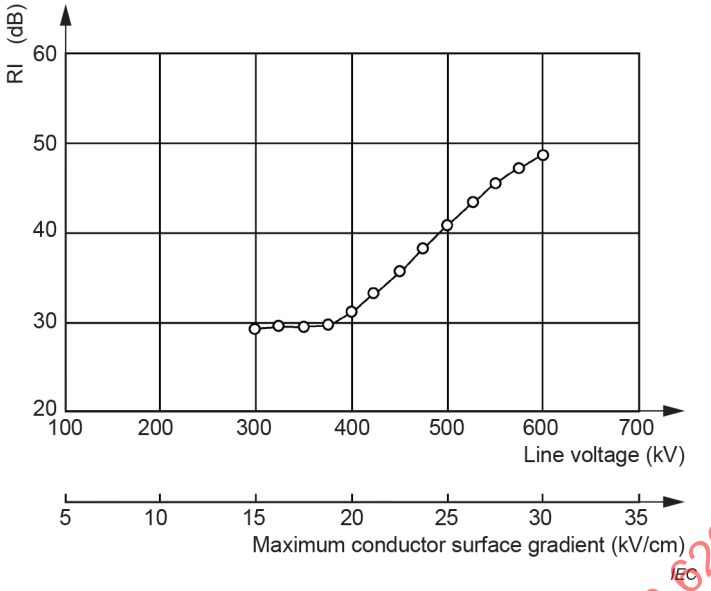

Figure B.4 – RI at 0,834 MHz as a function of bipolar line voltage 4 × 30,5 mm conductor, 11,2 m pole spacing, 15,2 m average height

RI in dB tends to be a linear function of conductor gradient and there is a slight roll-off tendency at the higher gradient which may be an indication of saturation. The inception of ionization usually occurs at around 14 kV/cm calculated maximum conductor surface gradient. But the beginning of line RI was observed from approximately 18 kV/cm, because ambient noise masked the actual corona inception level.

B.1.4 Percent cumulative distribution

As was pointed out in discussion of Figure B.5 to Figure B.8, the RI of DC transmission lines almost always decreases during rain. RI during rainy weather decreases by about 3 dB from the fair-weather level. However, a slight increase in RI was observed at the beginning of rain and with dry snow.

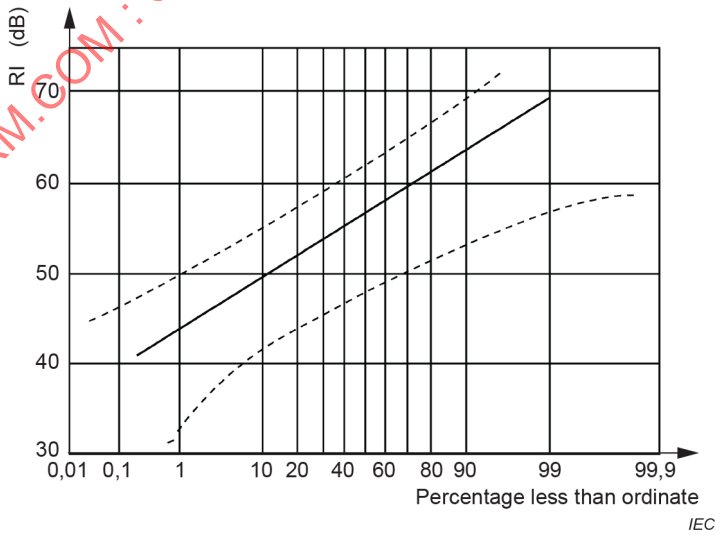

Figure B.5 – Percent cumulative distribution for fair weather, 2 × 46 mm, 18,3 m pole spacing, ±600 kV

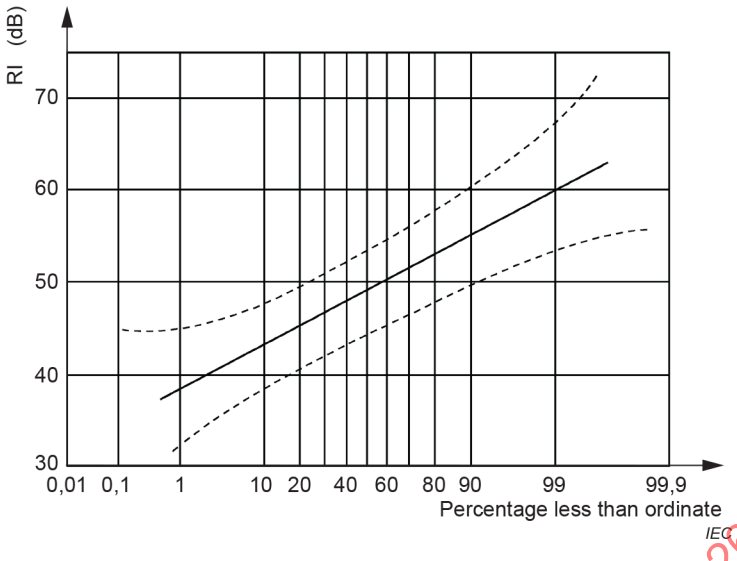

Figure B.6 – Percent cumulative distribution for rainy weather, 2 × 46 mm, 18,3 m pole spacing, ±600 kV

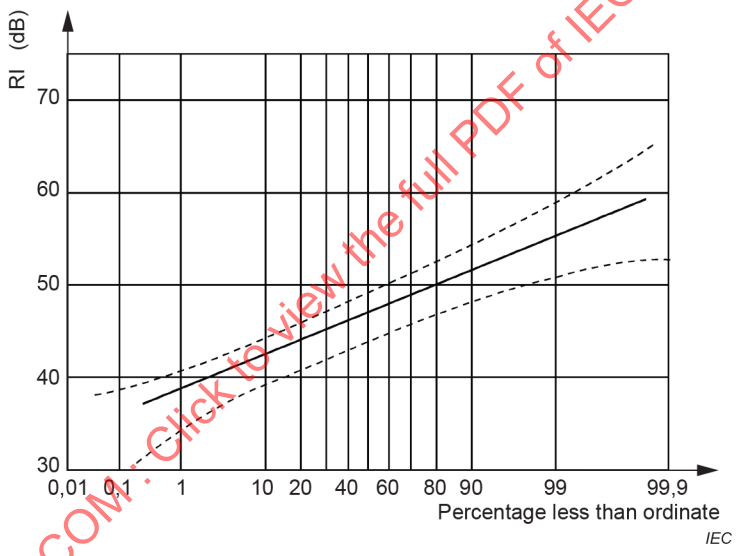

Figure B.7 – Percent cumulative distribution for fair weather, 4 × 30,5 mm, 13,2 m pole spacing, ±600 kV

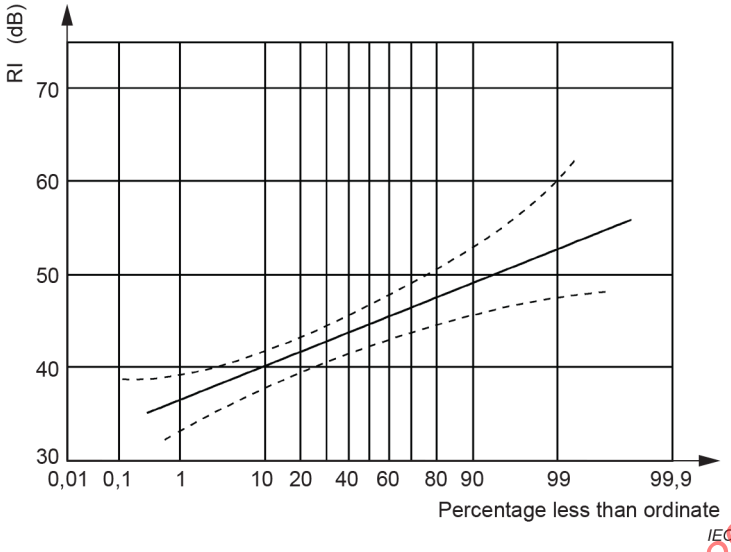

Figure B.8 – Percent cumulative distribution for rainy weather, 4 × 30,5 mm, 13,2 m pole spacing, ±600 kV

B.1.5 Influence of wind

Table B.1 compares the wind influence relationships obtained during this project with those obtained by other investigators.

Those data infer that all bipolar DC transmission lines operating above the critical level are influenced to about the same degree by wind, and that the maximum influence occurs when the wind flow is from negative to positive.

Table B.1 – Influence of wind on RI

Reference	Wind influence in dB/m/s	Description
BPA DC test project	0,8 [maximum] 0,3 [minimum]	±500 kV, Normal component – to + ±600 kV, Normal component – to + (Fair weather)
Other data	1,05 0,5	±400 kV, Wind – to + ±400 kV, Wind – to + (Probably all weather)
	1,1[maximum] 0,1[minimum]	±400 kV, Wind direction not considered (Probably all weather)
	0,9 0,2	±400 kV, Wind – to + ±400 kV, Winds other than – to + (Probably all weather)+

B.1.6 Spectrum

RI spectrum analyses were performed at the mid-span of Line Section 2 (4 × 30,5 mm, 11,2 m pole spacing) for both monopolar and bipolar operation at 400 kV to 600 kV. Spectrum measurements were made at 30,5 m (radial) from the positive polarity conductor. Figure B.9 illustrates the frequency spectrum for ±600 kV operation of the Test Line. As illustrated in the figure, the RI level of DC transmission line decreases about 8 dB for each doubling of frequency through the broadcast (AM) band.

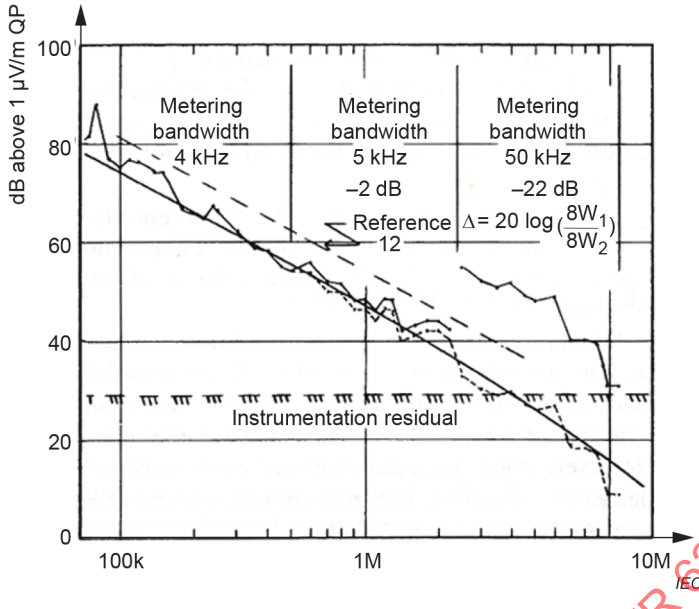

Figure B.9 – Radio interference frequency spectrum

RI vs. frequency at ±400 kV is shown in Figure B.10. These data were taken in line section 2 because it had the highest noise level. Figure B.10 presents the combined RI from all line sections including the wood-pole section.

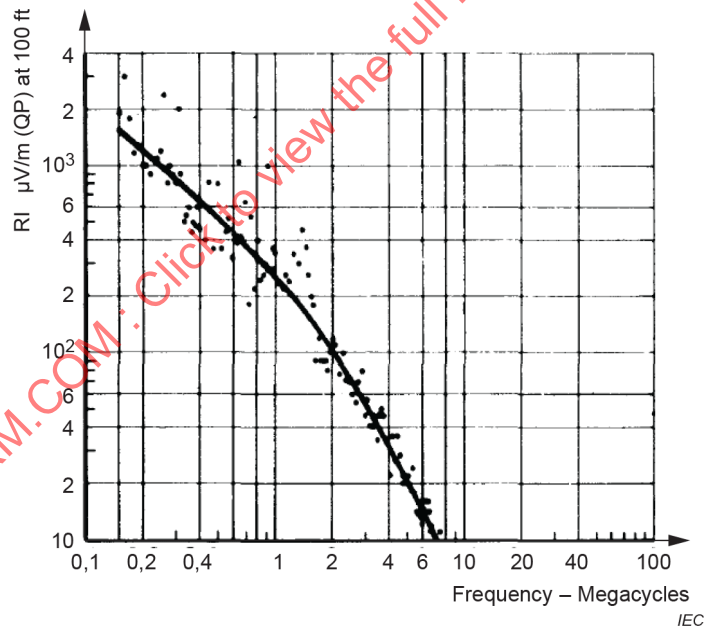

Figure B.10 – RI vs. frequency at ±400 kV [124]

In Figure B.10, RI measurements at 834 kHz were about 20 % lower than the mean frequency curve. This figure agreed closely with the correction factor for line section 2 longitudinal standing waves. The plot of RI vs. frequency, like that for AC lines, showed little RI above 10 MHz. Television interference meters could not detect interference except under the conductors at voltages above ±500 kV.

B.2 Hydro-Québec institute of research

B.2.1 General

Researchers from Hydro-Québec Institute of Research had provided detailed data about corona performance of a conductor bundle for bipolar HVDC transmission at ±750 kV [125]. The corona performance of a 4 mm × 40,6 mm conductor bundle has been studied on an outdoor test line at a nominal voltage of ±750 kV. The conductor bundle has been tested over a period of about six months covering summer, autumn and winter conditions.

B.2.2 Cumulative distribution

The results of long-term measurements made at ±750 kV were used to predict the statistical corona performance of a long line over a period of one year. All measured data had been converted to the case of a long line, using the same conductor bundle and having the same pole spacing and conductor height as the test line. Figure B.11 shows the cumulative distribution curves for RI.

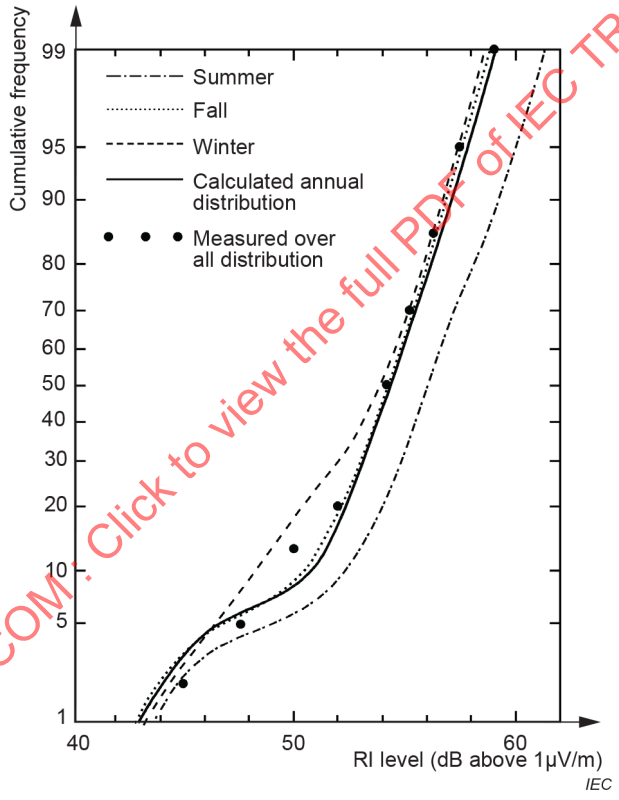

Figure B.11 – Cumulative distribution of RI measured at 15 m from the positive pole [125]

Table B.2 shows the statistical representation of the long-term RI performance of the tested conductor bundle. μ, σ and $\%T$ represent respectively the mean value, the standard deviation and the percentage time of each component distribution.

Table B.2 – Statistical representation of the long term RI performance of the tested conductor bundle [125]

Parameter		Fair weather			Foul weather		
		μ	σ	$\%T$	μ	σ	$\%T$
RI	Summer	55,9	2,0	94,4	45,6	2,3	5,6
	Autumn	53,6	1,8	93,0	45,5	2,6	7,0
	Winter	54,0	2,2	91,0	45,3	1,9	9,0
	Annual	54,4	1,95	92,85	45,47	2,36	7,15

B.2.3 Spectrum

Figure B.12 showed the frequency spectra of RI which had been tested mostly under fair weather conditions.

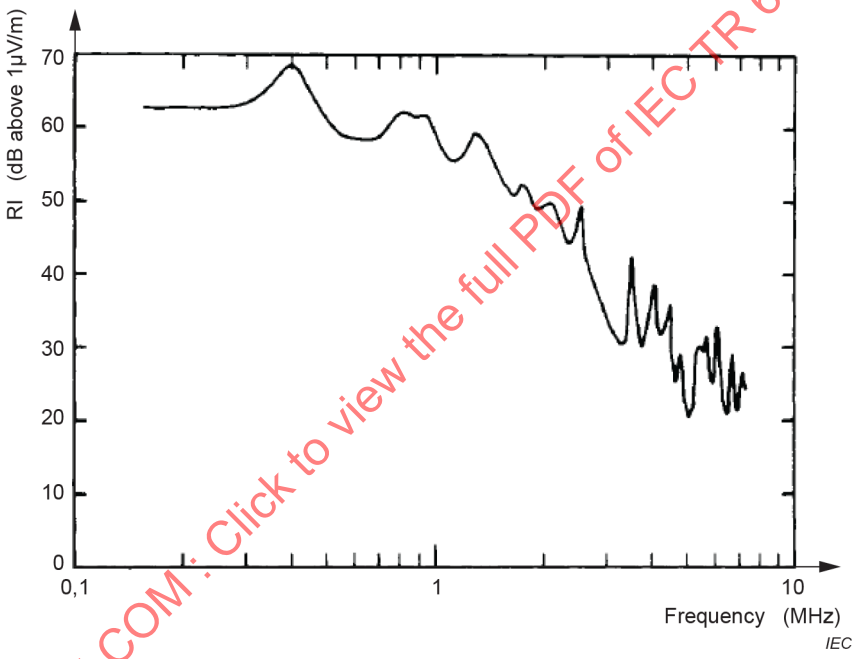

Figure B.12 – Conducted RI frequency spectrum measured with the line terminated at one end [125]

B.2.4 Lateral profiles

Figure B.13 showed the lateral profiles of RI which had been tested mostly under fair weather conditions.

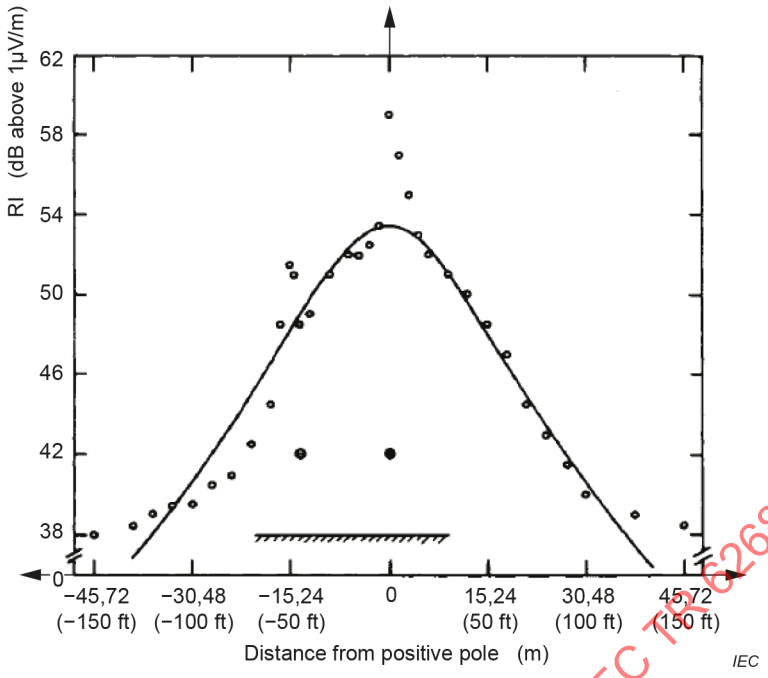

Figure B.13 – Lateral profile of RI [125]

B.3 DC lines of China

Table B.3 presents measured data from two ±500 kV DC lines in China. Calculations based on the CISPR recommended RI prediction formula for a bipolar line have also been listed in the table. The Guizhou-Guangzhou ±500 kV DC line uses 4 cm × 3,624 cm conductors, whereas the Tianshengqiao-Guangzhou ±500 kV DC line uses 4 cm × 2,628 cm conductors. The distance between location of measurement and the converter station is more than 100 km.

Table B.3 – RI at 0,5 MHz at lateral 20 m from positive pole (fair weather)

Measured line	Height from line to ground (m)	Altitude (m)	Measured value (dB/μV/m)	Calculated value (dB/μV/m)
Guizhou-Guangzhou ±500 kV DC line	15,7	1 450	48,7	46,0
	16,7	500	43,8	45,6
Tianshengqiao-Guangzhou ±500 kV DC line	15,2	11	47,4	49,0
	14,7	24	47,6	49,1

China has also built up HVDC test lines. The lateral profile of RI field strength (50 % value) is given in Figure B.14, together with the calculation result by empirical formula of CISPR and American EPRI. Figure B.14 shows that the 50 % value for RI is 47,3 dB (μV/m) at the reference point, when conductor with 6 × 720 mm^2 pattern of, 18 m height, and 22 m pole spacing are adopted for the ±800 kV DC test lines. It could be seen that the calculation result of CISPR empirical formula is closer to the test result.